Supplementary information for manuscript

The contribution of wood burning and other pollution sources to wintertime organic aerosol levels in two Greek cities

Kalliopi Florou[1,2], Dimitrios K. Papanastasiou[1,2], Michael Pikridas[1,2], Christos Kaltsonoudis[1,2], Evangelos Louvaris[1,2], Georgios I. Gkatzelis[1,2], David Patoulias[1,2], Nikolaos Mihalopoulos[3,4], and Spyros N. Pandis[1,2,5]

[1]Institute of Chemical Engineering Sciences, ICE/FORTH, Patras, Greece,

[2]Department of Chemical Engineering, University of Patras, Patras, Greece,

[3]Department of Chemistry, University of Crete, Greece

[4]IERSD, National Observatory of Athens, Athens, Greece

[5]Department of Chemical Engineering, Carnegie Mellon University, Pittsburgh, USA

Correspondence to: Spyros N. Pandis (spyros@chemeng.upatras.gr)

1. Location of sampling sites

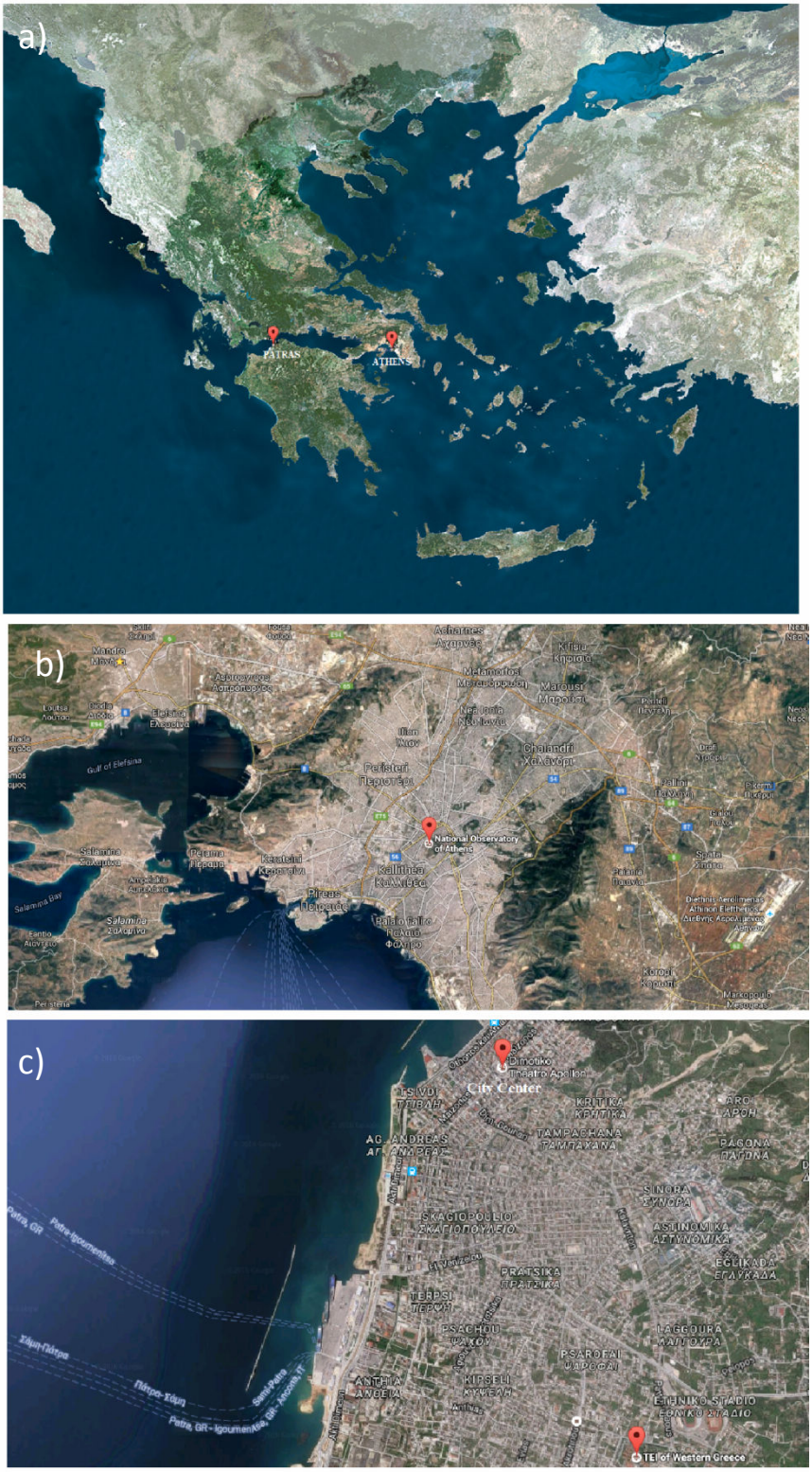

Figure S1. The location of the sampling sites: (a) the cities of Patras and Athens in Greece; (b) the National Observatory (Thiseio) in Athens; and (c) the Technological Educational Institute (TEI) and the city center of Patras.

2. Origin of air masses in Patras

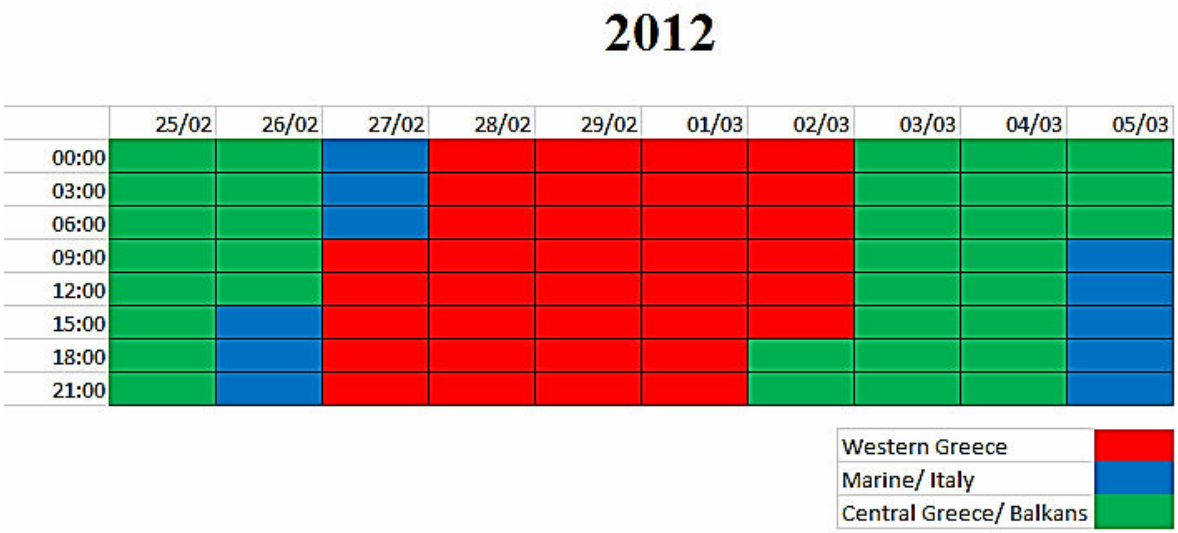

Figure S2. FLEXPART analysis for the Patras campaign.

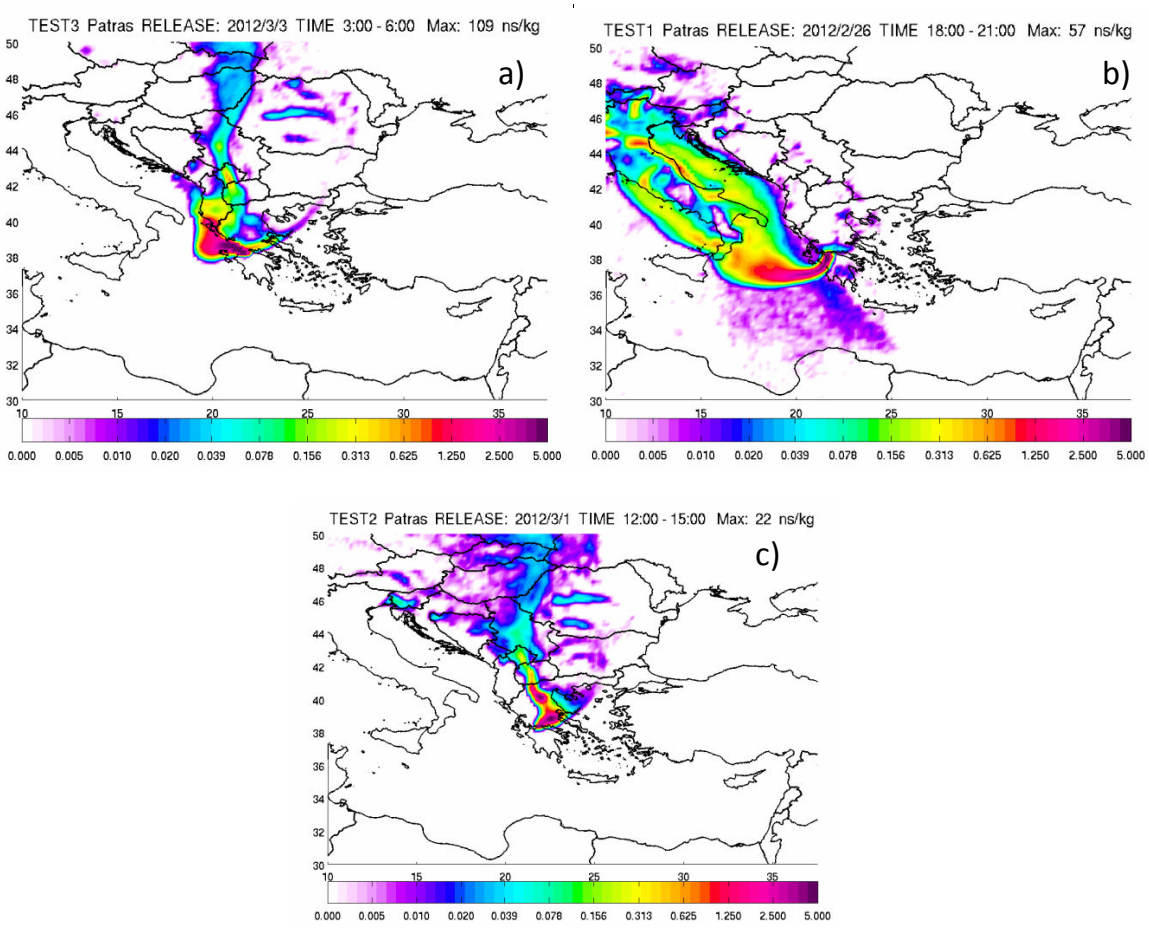

Figure S3. Examples of the three categories of back-trajectories of air masses arriving in Patras: a) western Greece; b) marine/Italy; and c) central Greece/Balkans.

3. Origin of air masses in Athens

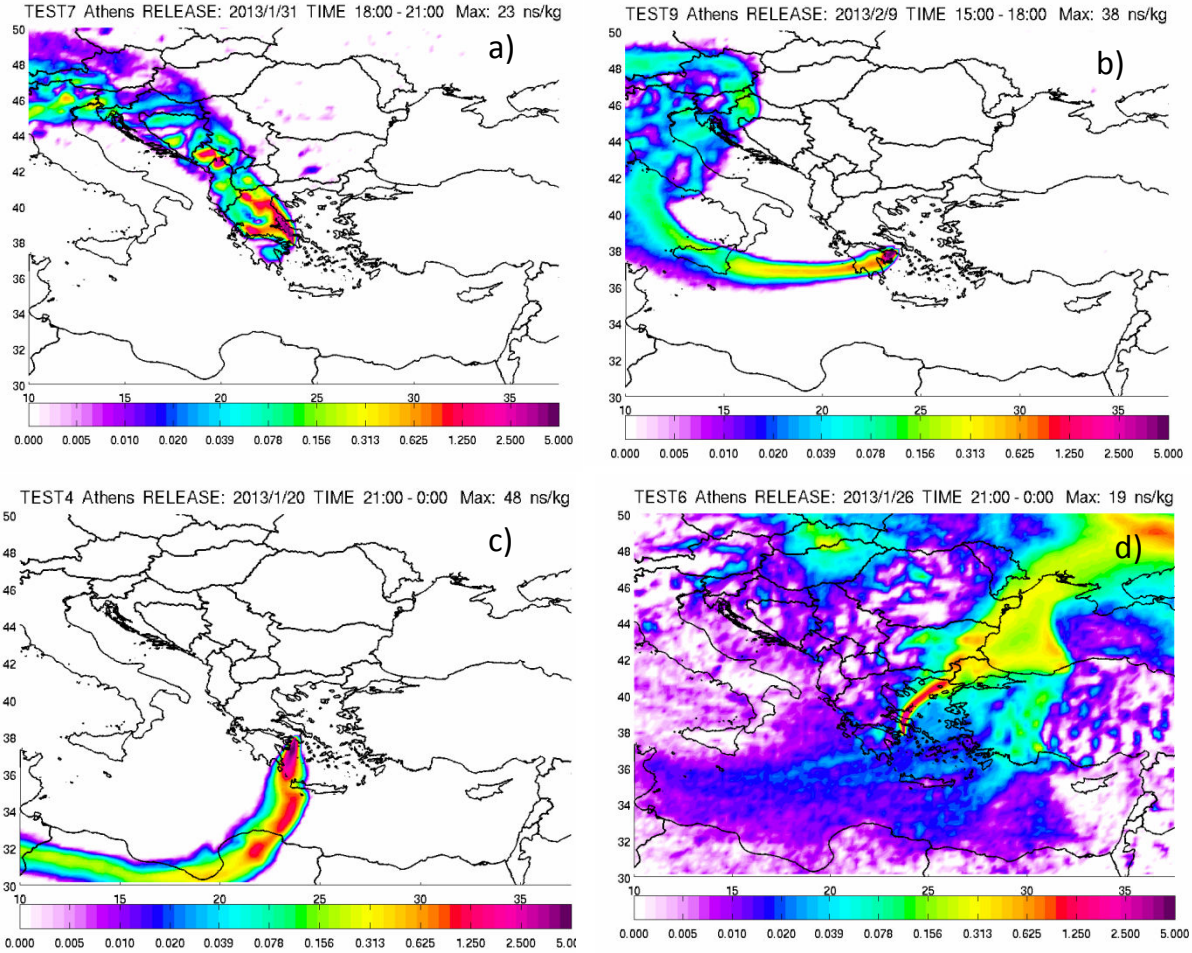

Figure S4. Examples of the three categories of back-trajectories of air masses arriving in Athens: (a) Greece-Balkans; (b) marine (Sicily); (c) Africa and (d) Aegean/NE.

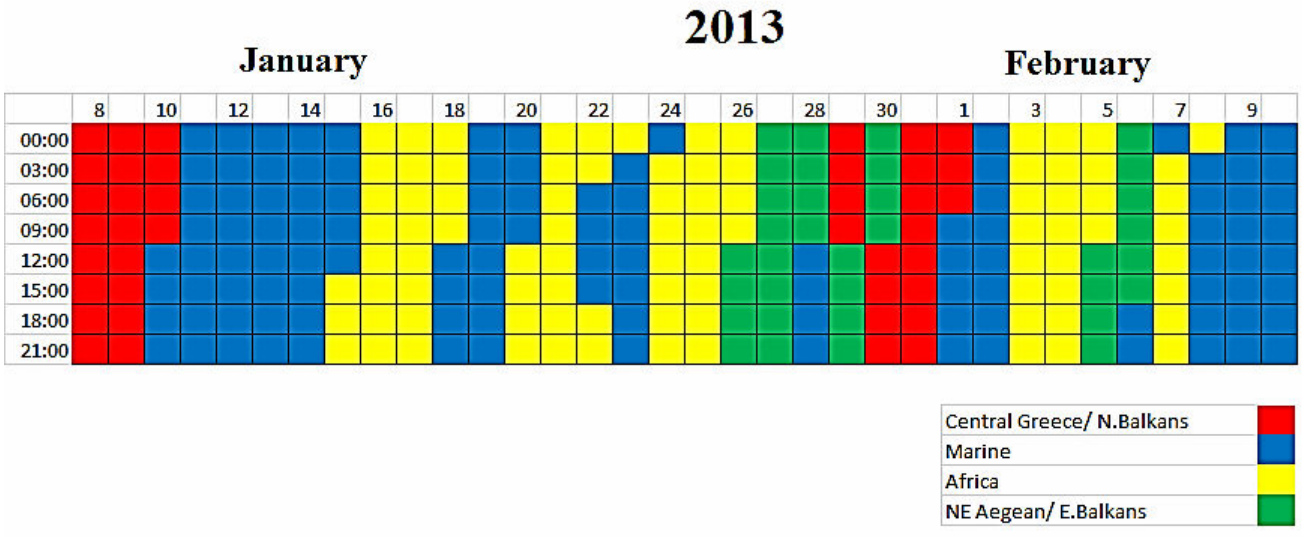

Figure S5. FLEXPART analysis for the Athens campaign.

4. Rain events in Athens

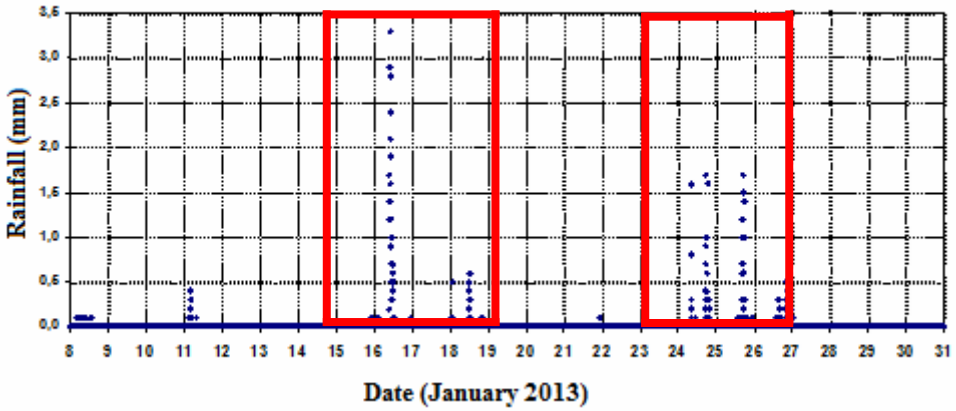

Figure S6. Cumulative precipitation at 5-min intervals in the center of Athens during January 2013.

5. Average AMS size distributions

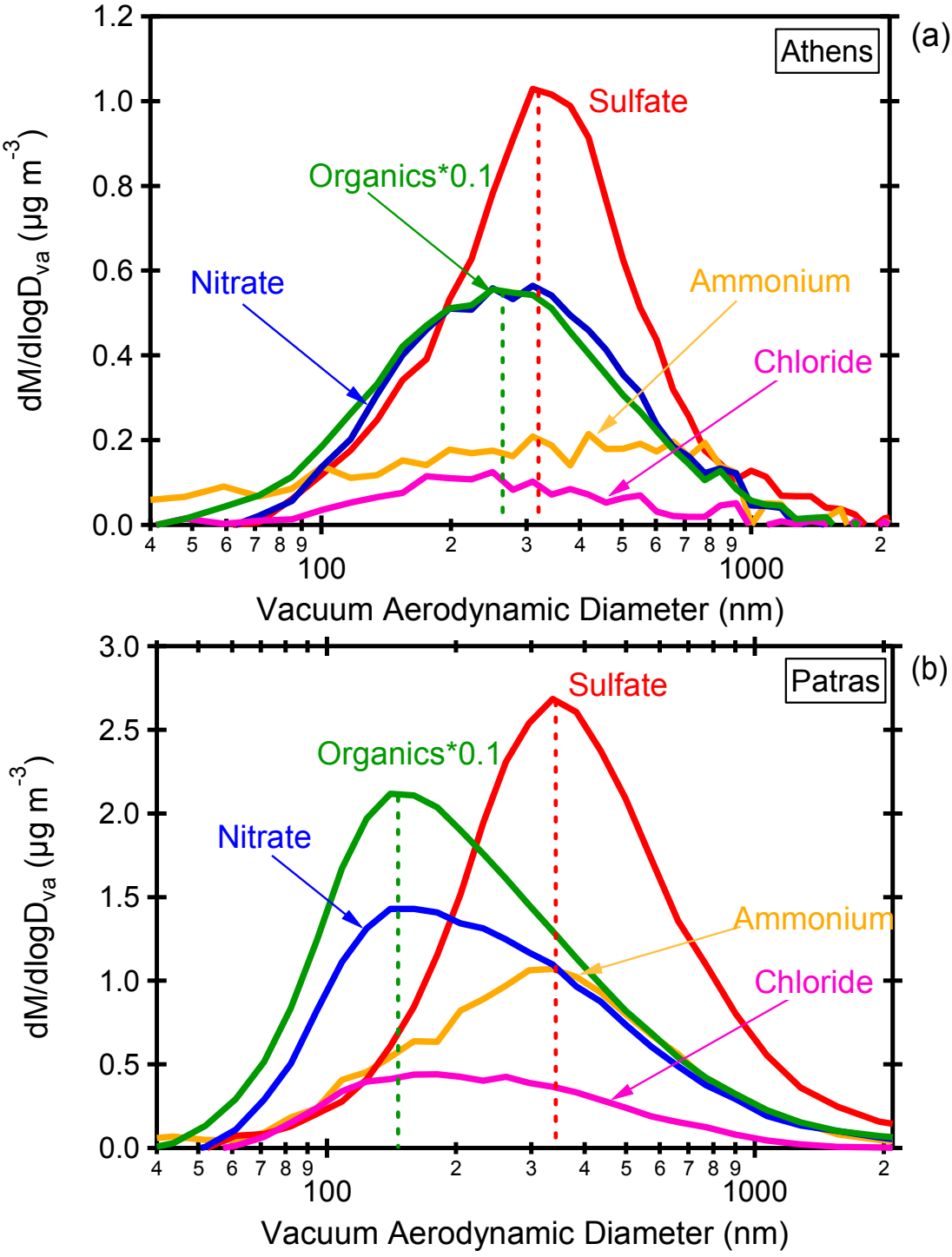

Figure S7. The average HR-AMS size distributions as a function of vacuum aerodynamic diameter for: (a) Athens and (b) Patras. The modes of the size distribution of the organics and sulfates are marked with dashed lines.

6. Elemental ratios and carbon oxidation state (OS_C)

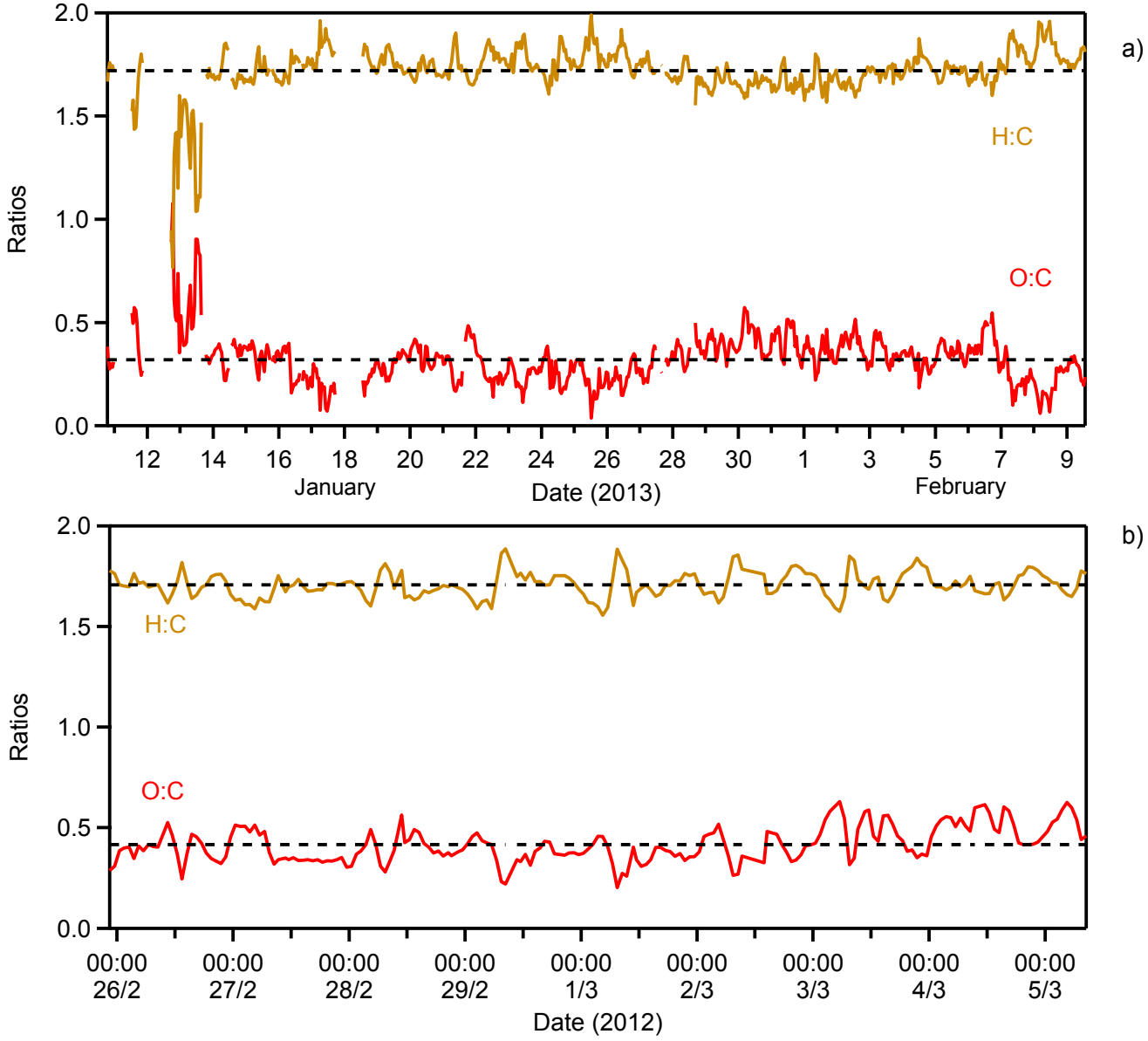

Figure S8. Time series of the OA O:C and H:C ratios for: a) Athens and b) Patras based on the approach of Canagaratna et al. (2015).

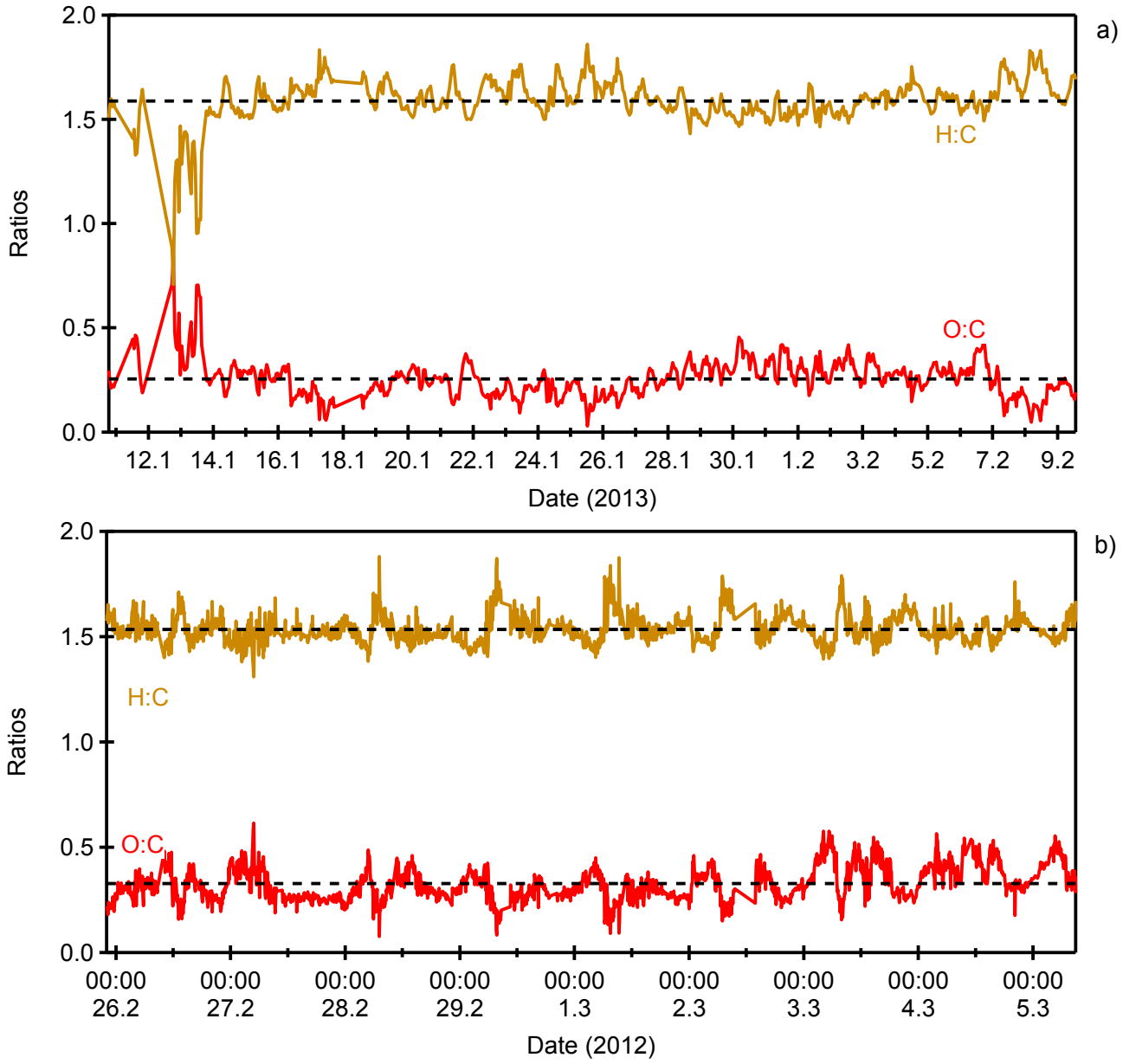

Figure S9. O:C and H:C elemental ratios in: a) Athens and b) Patras, based on the approach of Aiken et al. (2008).

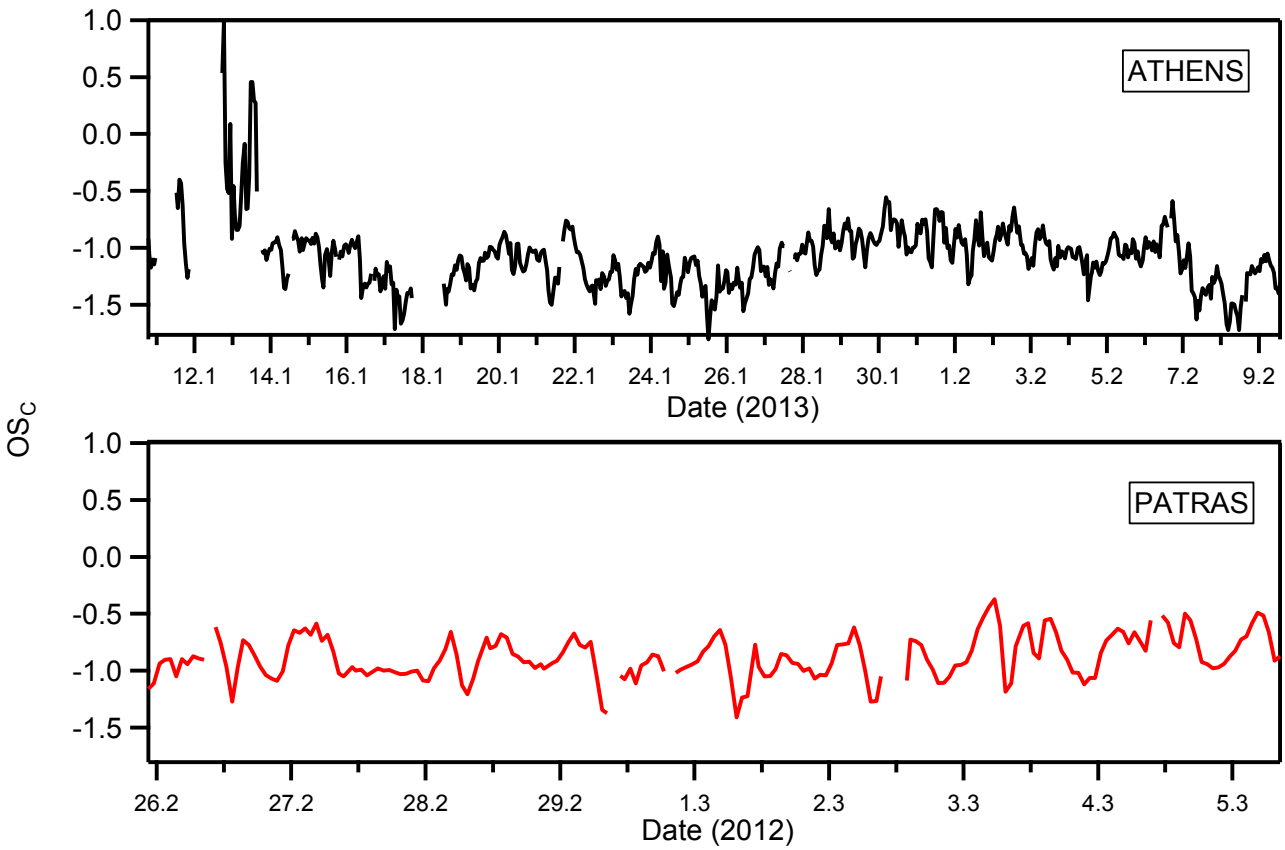

Figure S10. Average carbon oxidation state OS_C for the two cities.

7a. PMF solution choice for Patras

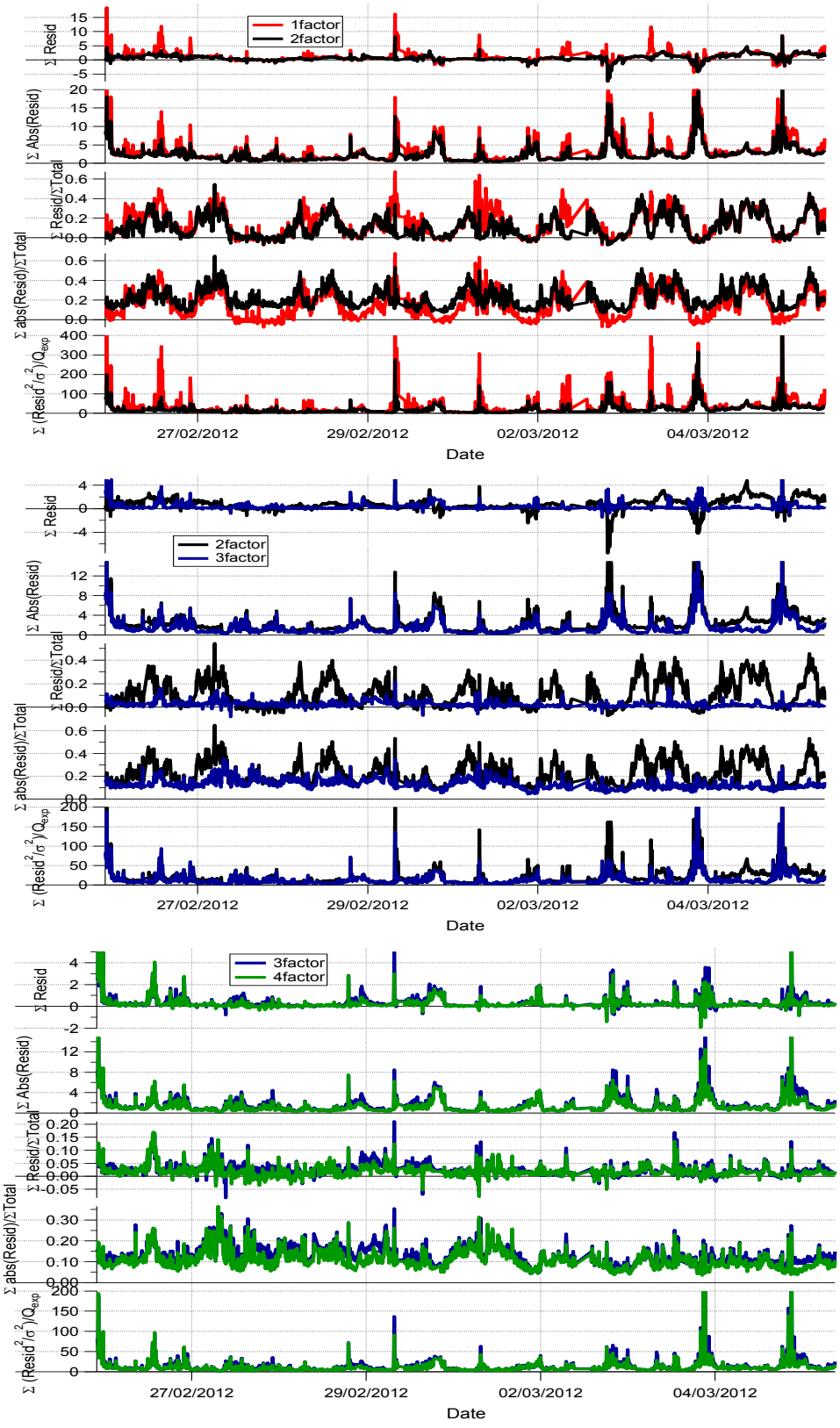

Figure S11. Model residuals **E= X-GF** calculated using the PMF evaluation tool PET (Ulbrich et al., 2009) for Patras. Comparison between (a) 1-factor (red lines) and 2-factor (black lines) PMF solutions, (b) 2-factor (black lines) and 3-factor (blue lines) PMF solutions, and (c) 3-factor (blue lines) and 4-factor (green lines) PMF solutions.

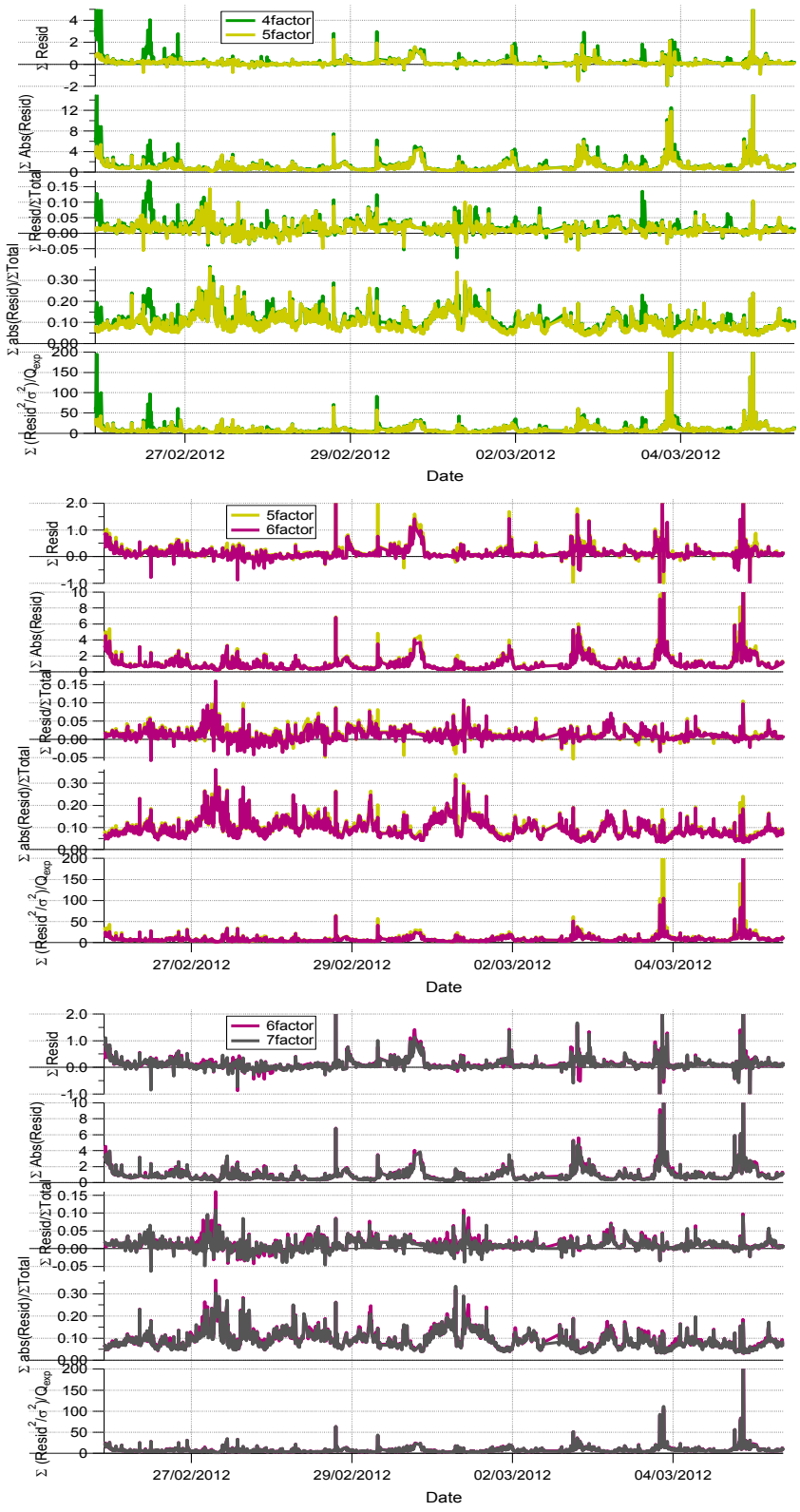

Figure S12. Model residuals **E=X-GF** calculated using the PMF evaluation tool PET (Ulbrich et al., 2009) for Patras. Comparison between a) 4-factor (green lines) and 5-factor (yellow lines) solutions, (b) 5-factors (yellow lines) and 6-factors (pink lines), and (c) 6-factors (pink lines) and 7-factors (grey lines) PMF solutions. The residuals decreased from 4 to 5 factors especially for the first days of the campaign and March 4. The 5, 6 and 7 factor solution residuals were almost identical.

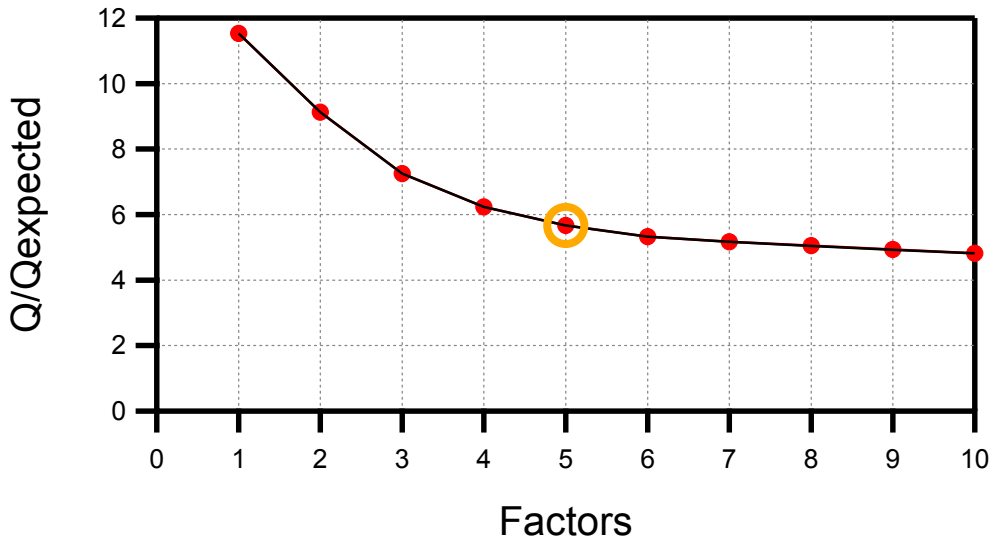

Figure S13. $Q/Q_{expected}$ vs. the number of the factors in Patras.

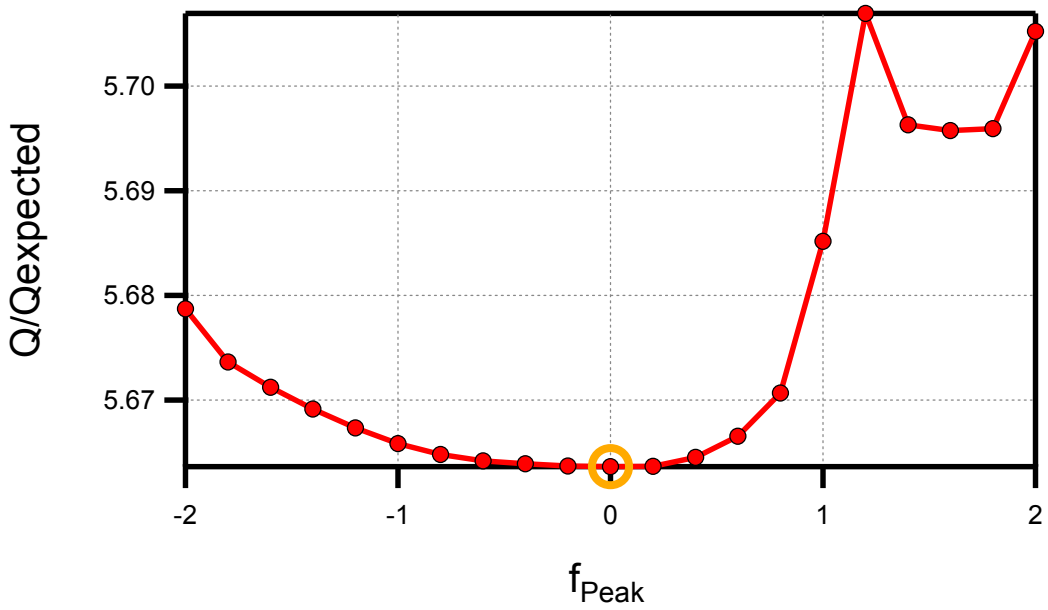

Figure S14. $Q/Q_{expected}$ for f_{peal} -2 to 2 for the 5-factor solution in Patras. There is a stable between f_{peak} -0.6 and 0.2, with the lower $Q/Q_{expected}$ at f_{peak}=0.0 and f_{peak}=0.2.

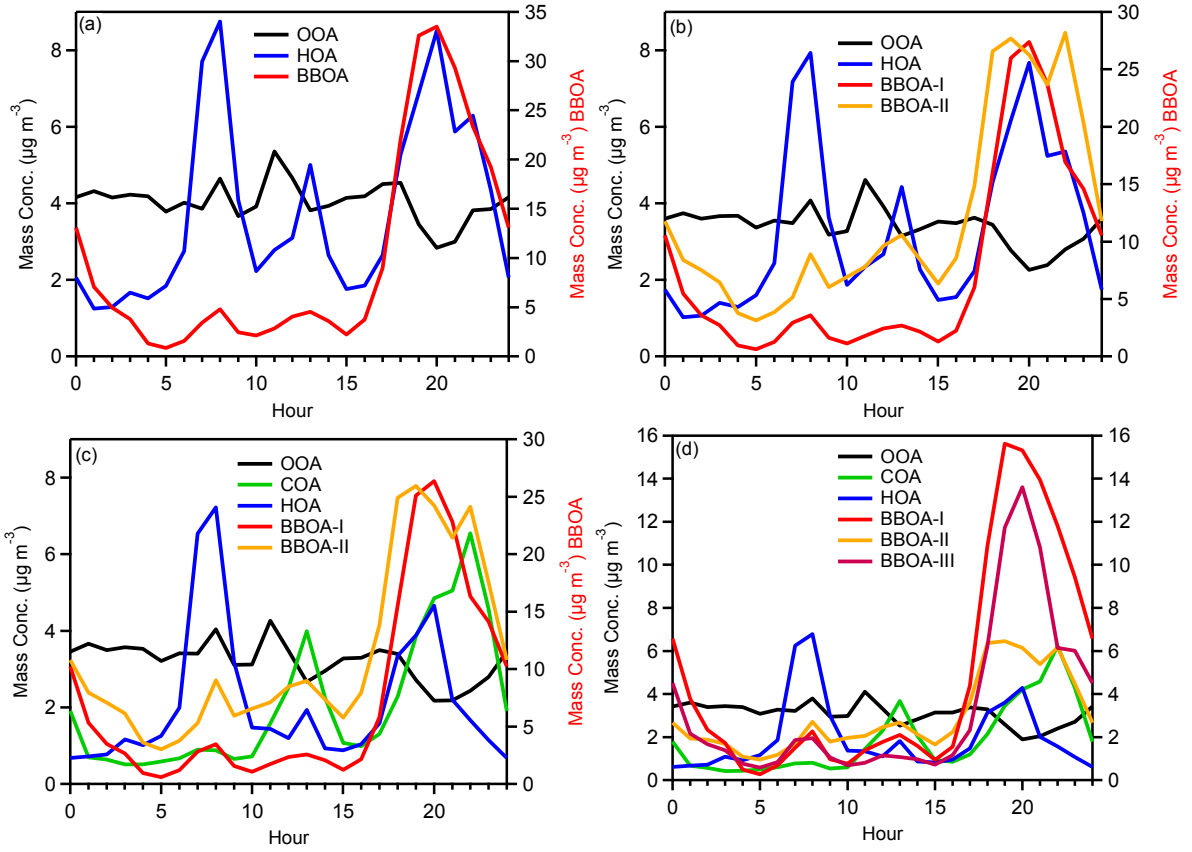

Figure S15. Average diurnal profiles of the mass concentration for the: (a) 3, (b) 4, (c) 5 and (d) 6 factor PMF solutions in Patras.

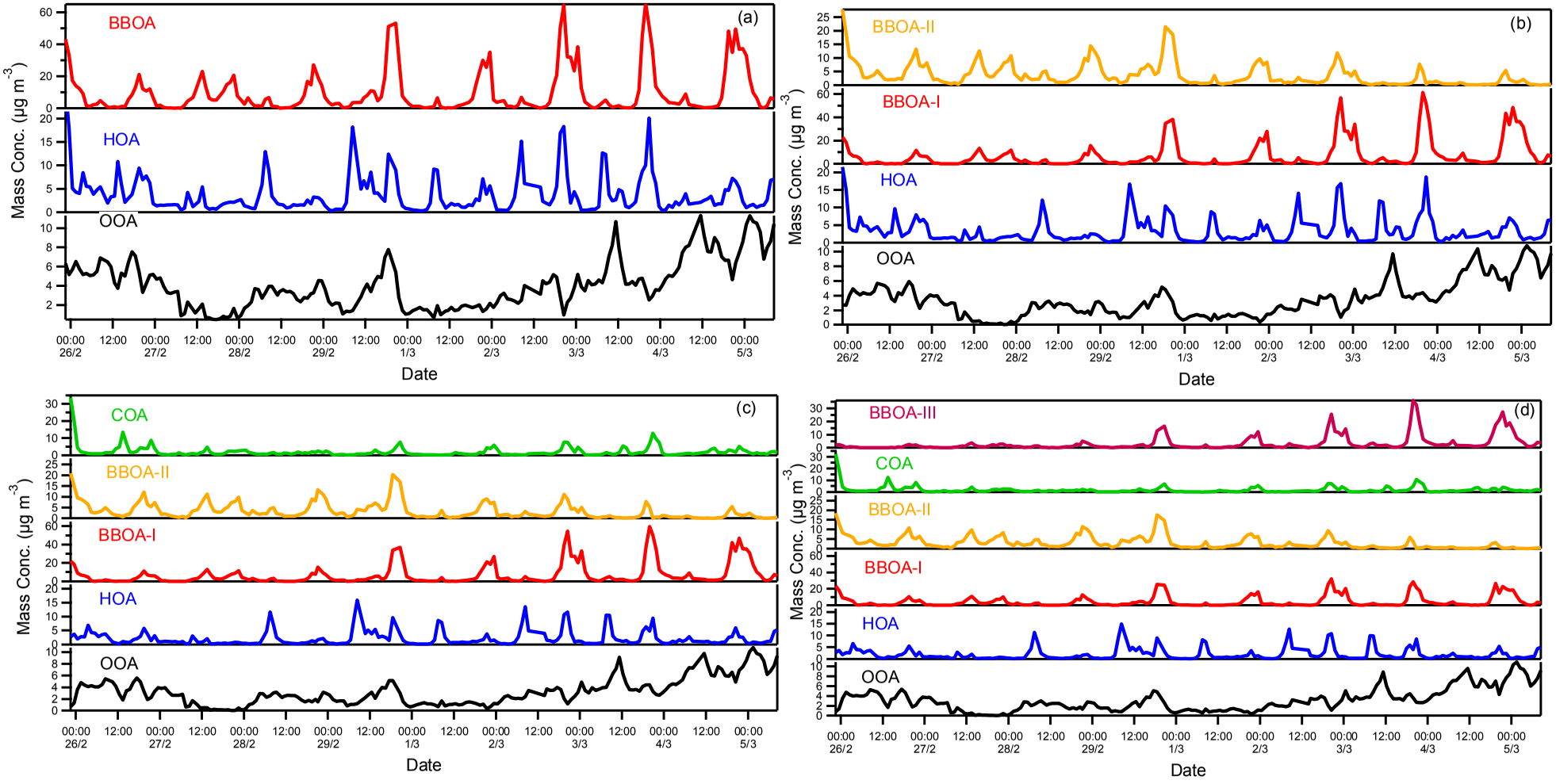

Figure S16. Time series for the: (a) 3, (b) 4, (c) 5 and (d) 6 factor PMF solutions in Patras.

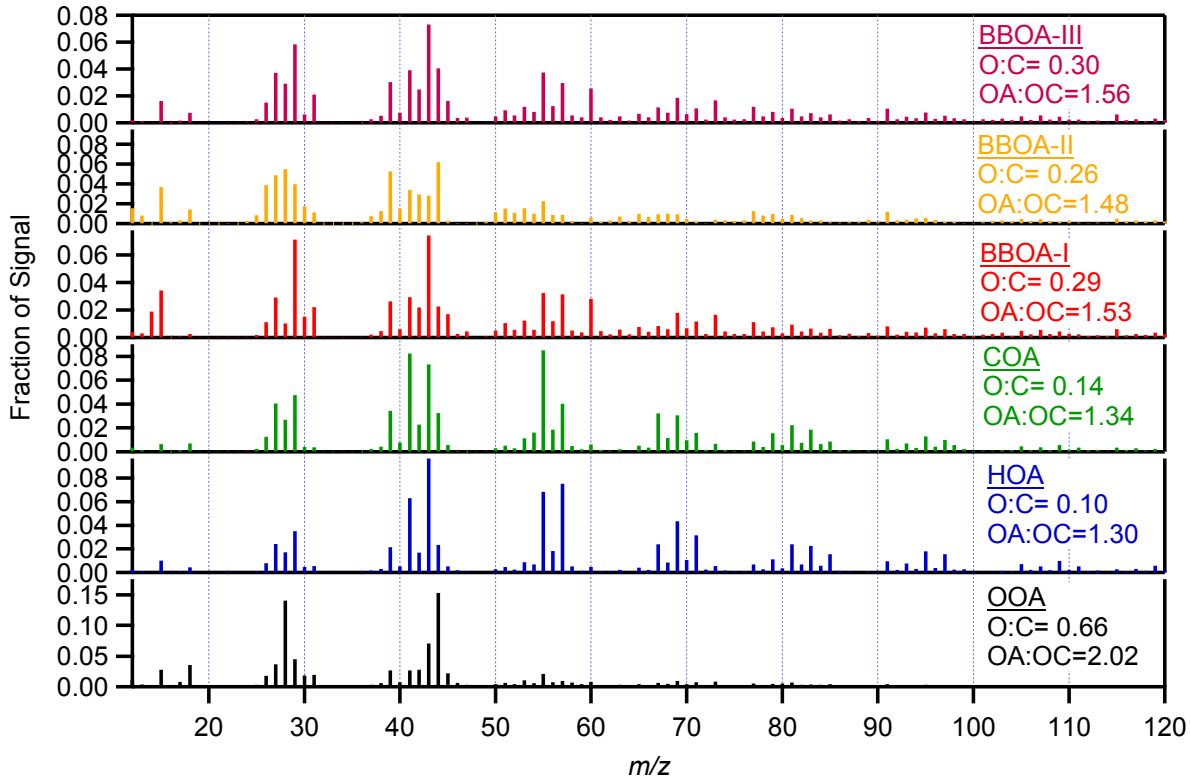
Fraction of Signal
m/z
BBOA-III
O:C= 0.30
OA:OC=1.56
BBOA-II
O:C= 0.26
OA:OC=1.48
BBOA-I
O:C= 0.29
OA:OC=1.53
COA
O:C= 0.14
OA:OC=1.34
HOA
O:C= 0.10
OA:OC=1.30
OOA
O:C= 0.66
OA:OC=2.02

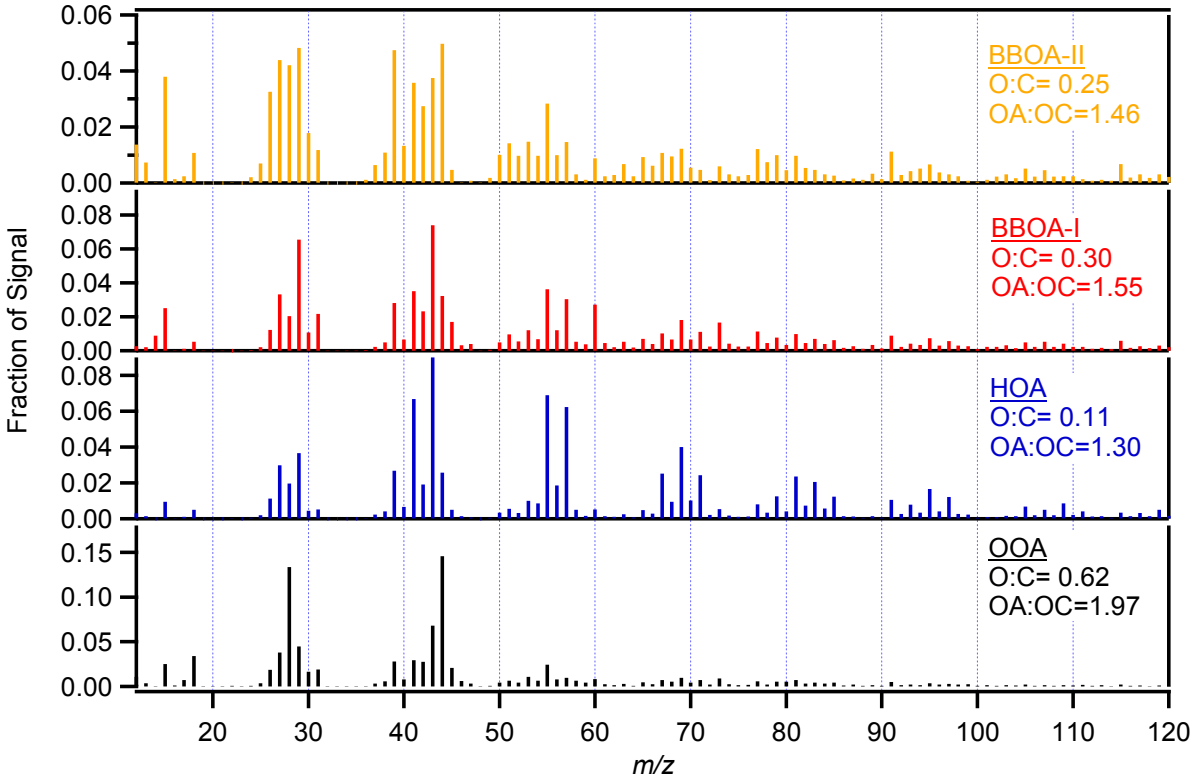
Fraction of Signal
m/z
BBOA-II
O:C= 0.25
OA:OC=1.46
BBOA-I
O:C= 0.30
OA:OC=1.55
HOA
O:C= 0.11
OA:OC=1.30
OOA
O:C= 0.62
OA:OC=1.97

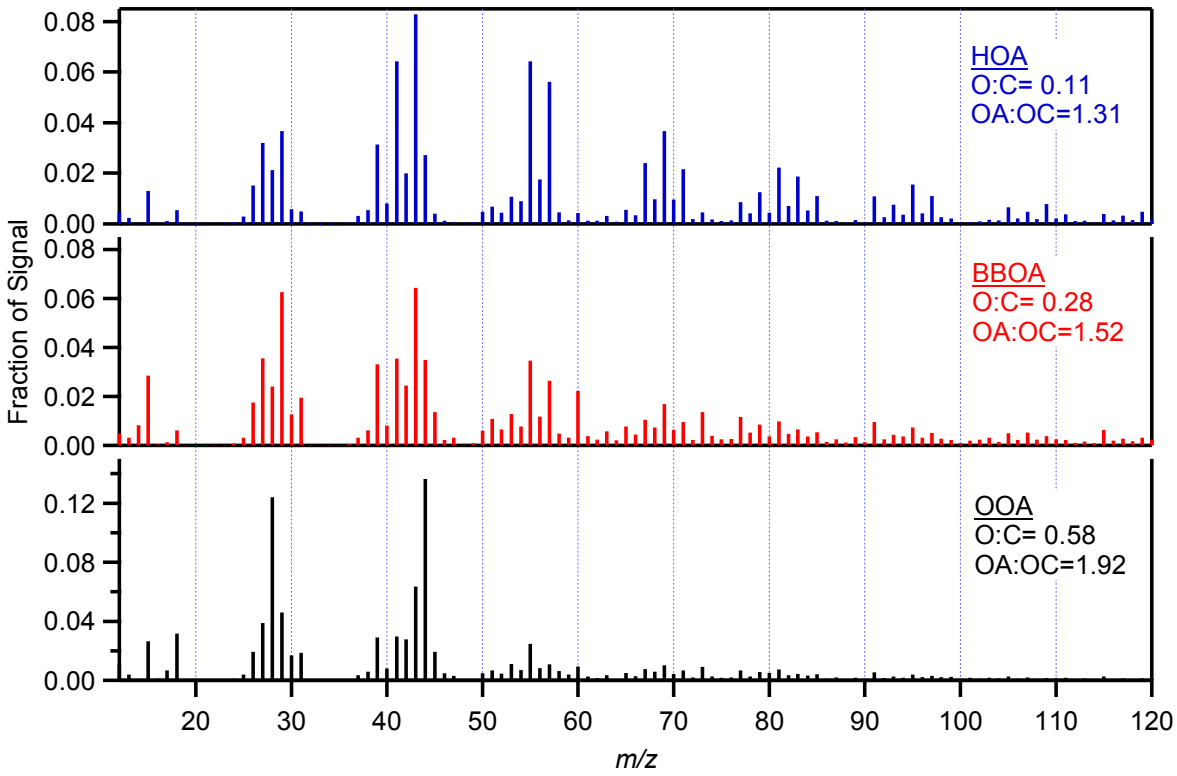

Figure S17. AMS spectra for the 6, 4 and 3-factor PMF solutions in Patras.

7b. PMF solution choice for Athens

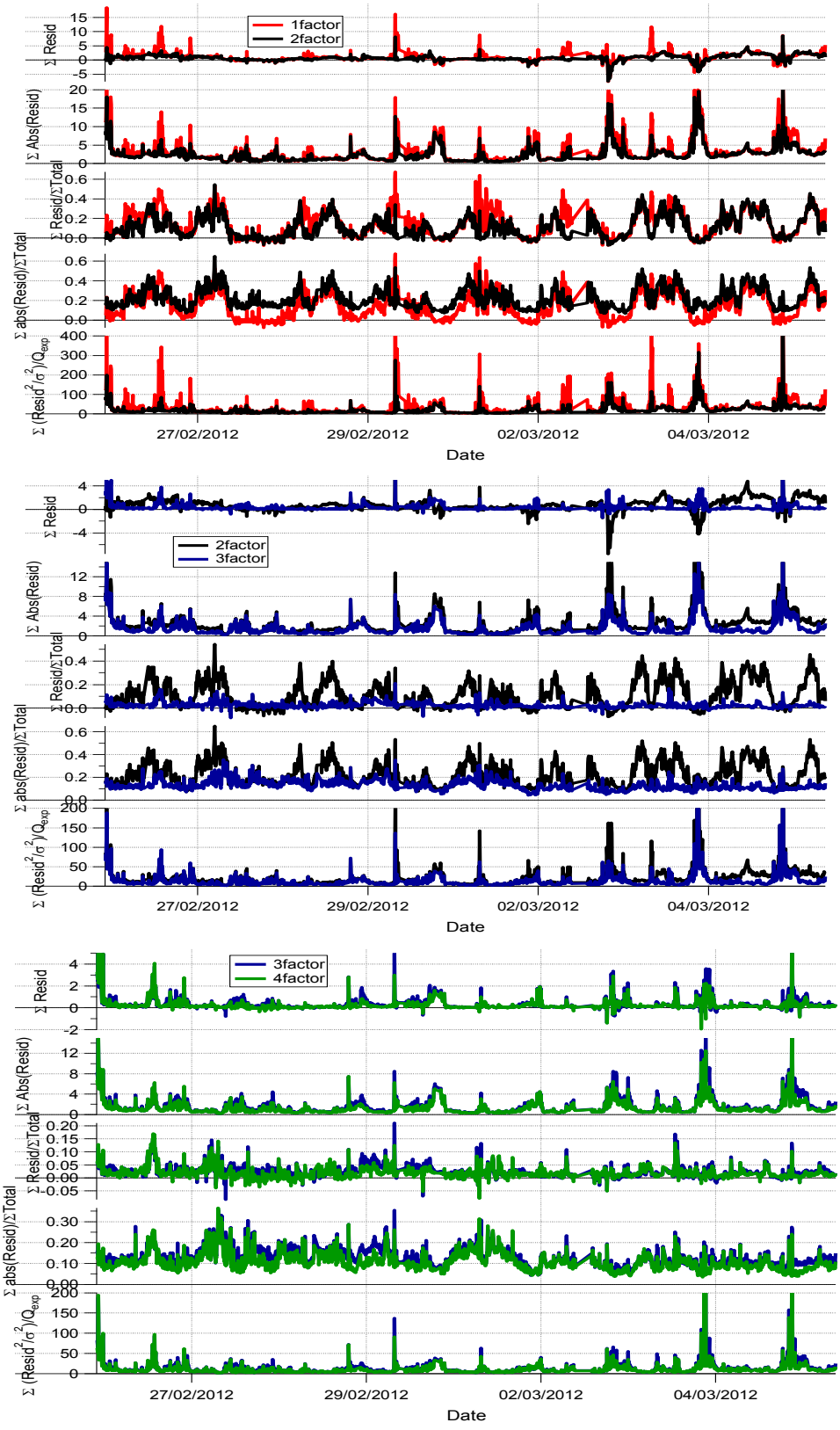

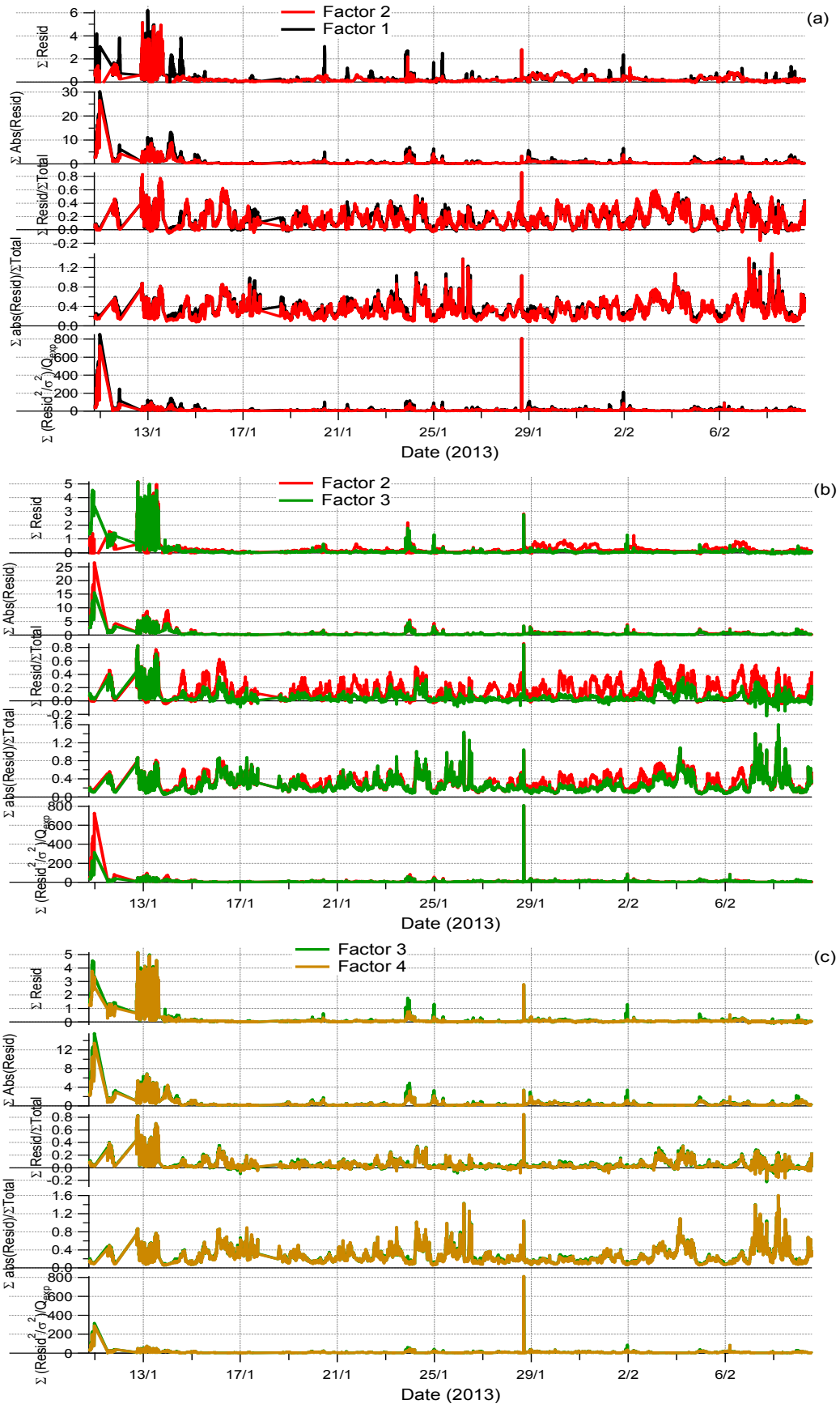

Figure S18. Model residuals **E= X-GF** calculated using the PMF evaluation tool, PET (Ulbrich et al., 2009) for Athens. Comparison between (a) 1-factor (black lines) and 2-factor (red lines) PMF solutions, (b) 2-factor (red lines) and 3-factor (green lines) PMF solutions, and (c) 3-factor (green lines) and 4-factor (yellow lines) PMF solutions.

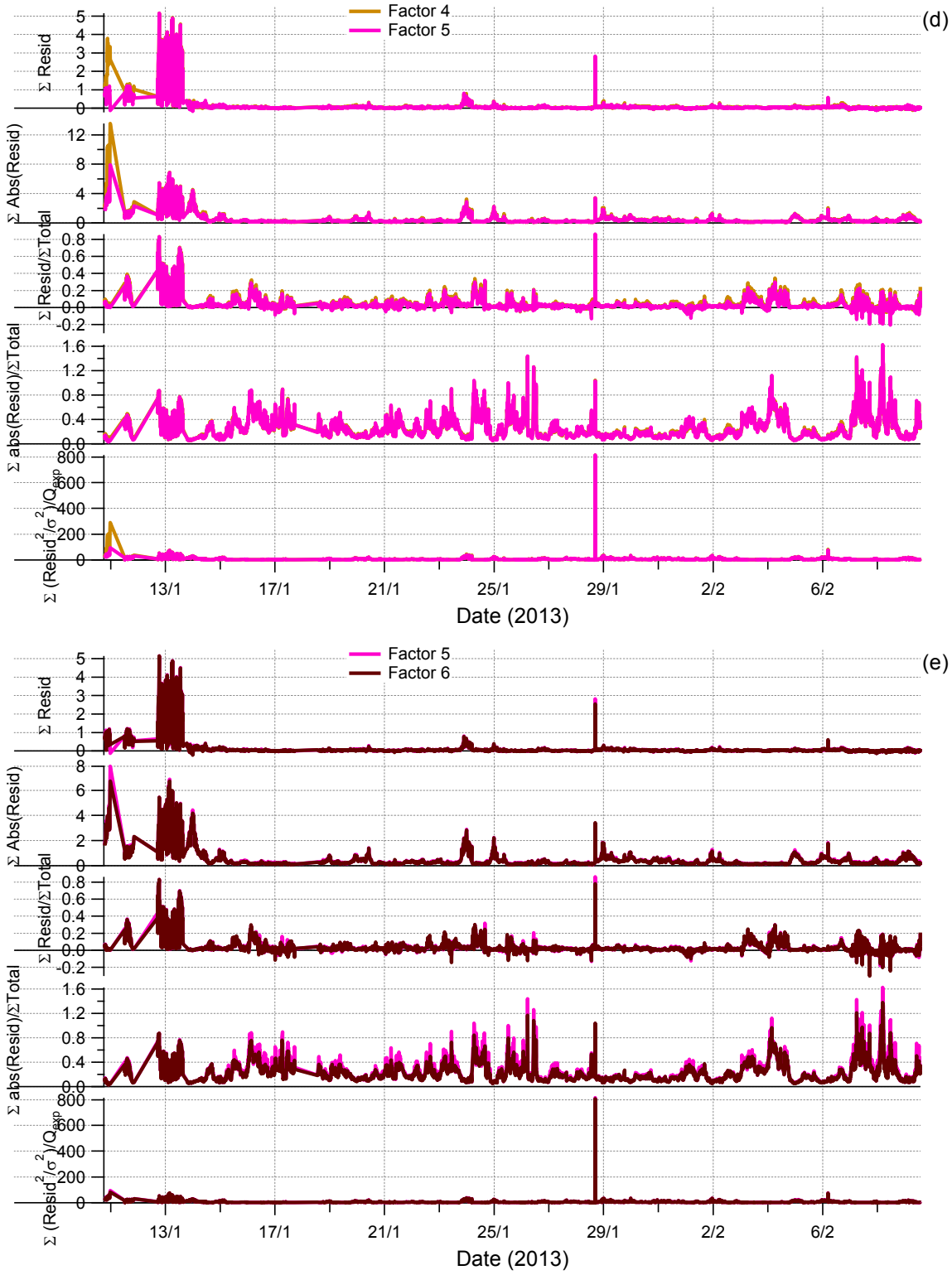

Figure S19. Model residuals **E=X-GF** calculated using the PMF evaluation tool, PET (Ulbrich et al., 2009) for Athens. Comparison between a) 4-factor (yellow lines) and 5-factor (pink lines) solutions, and (b) 5-factor (pink lines) and 6-factor (brown lines) PMF solutions.

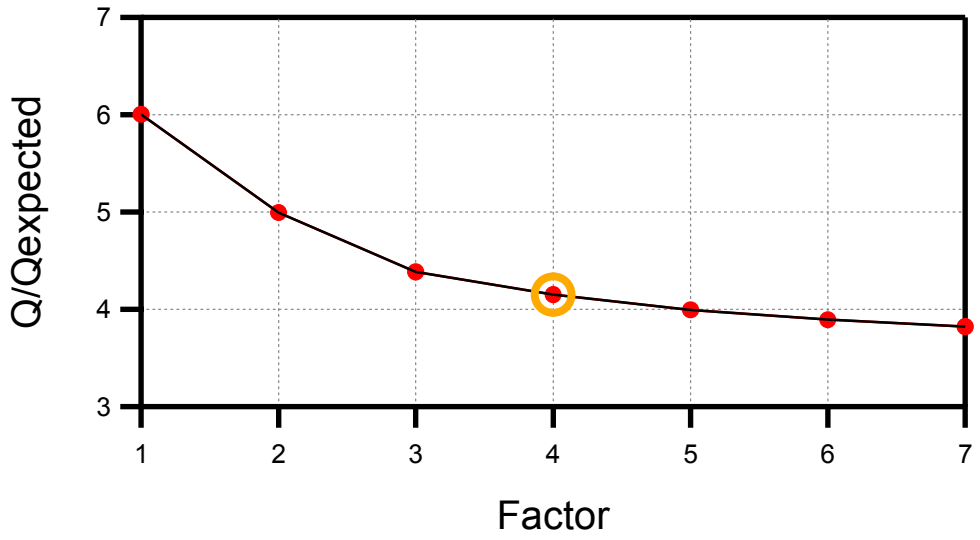

Figure S20. $Q/Q_{expected}$ vs. the number of the factors for Athens.

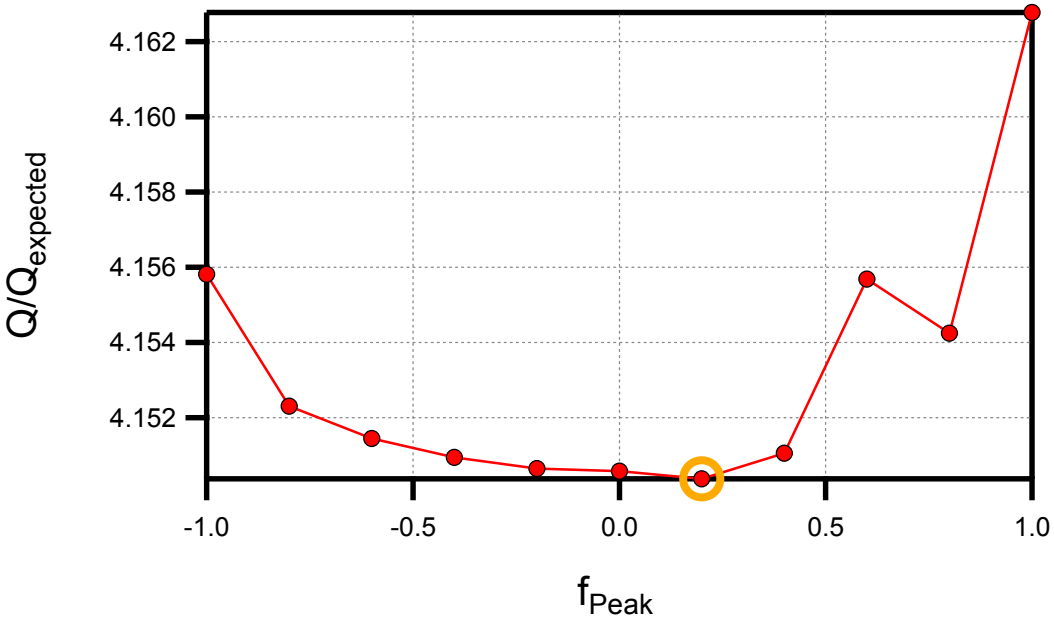

Figure S21. $Q/Q_{expected}$ for f_{peak} -1 to 1 for a 4 factor solution for Athens. There is a stable area between the f_{peak} -0.4 and 0.2, with the lower $Q/Q_{expected}$ at f_{peak}=0.2.

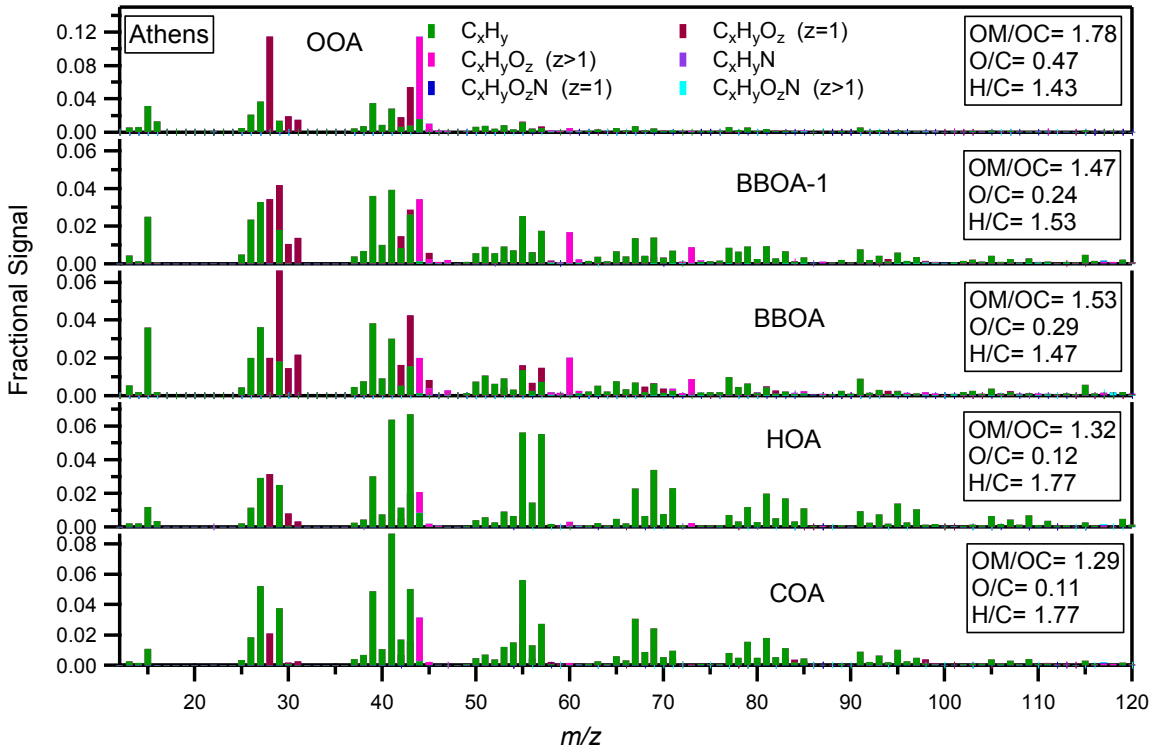

Figure S22. High resolution spectra by the AMS for the 5-factor PMF solution for Athens.

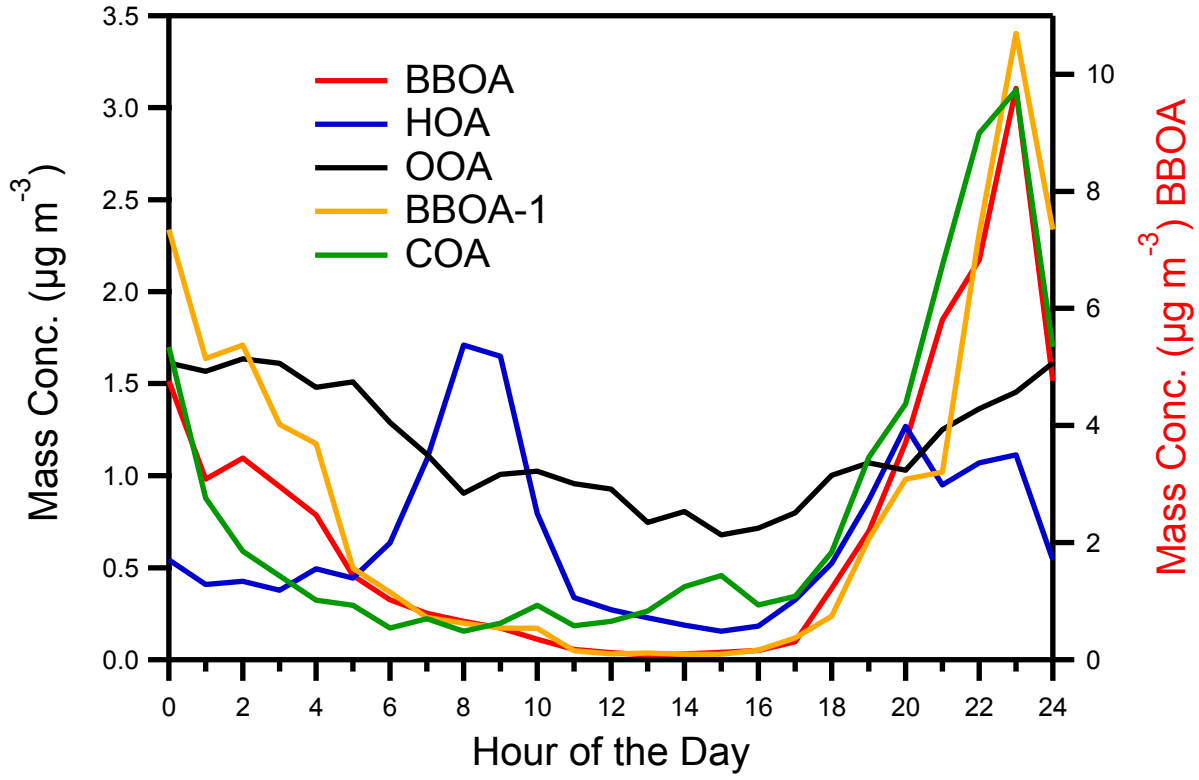

Figure S23. Diurnal profiles of the mass concentration for the 5 factor PMF solution in Athens. The BBOA mass concentration appears on the right y-axis.

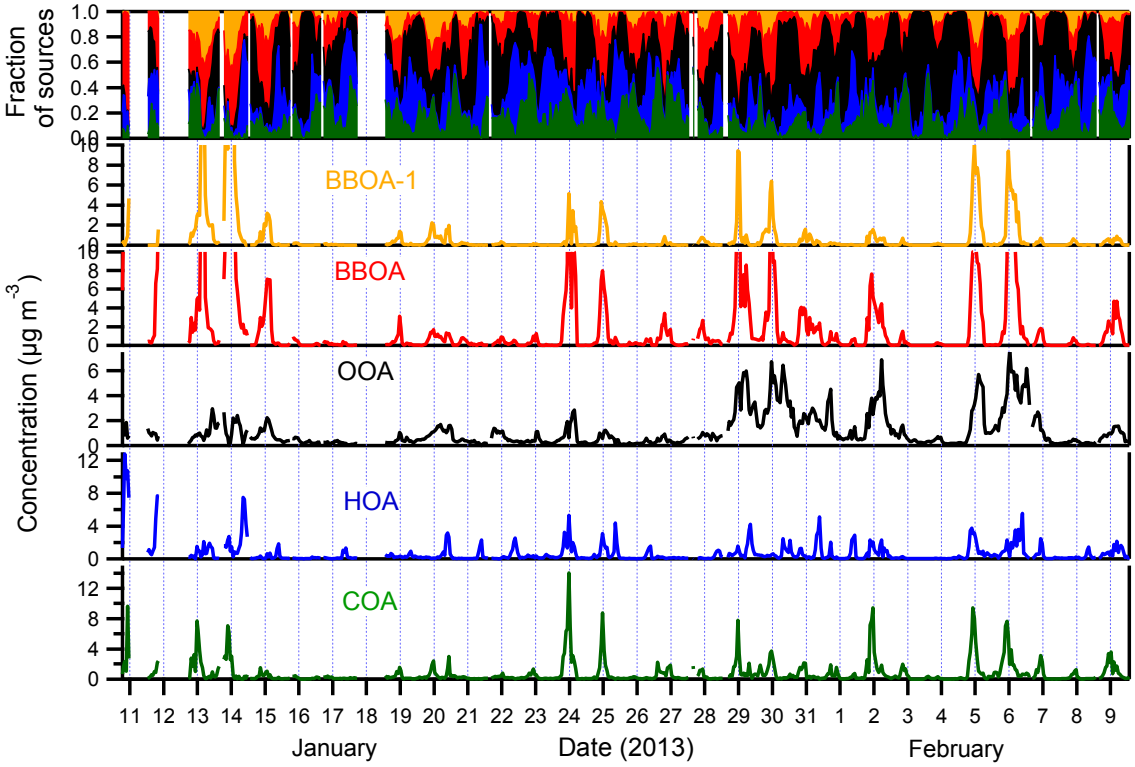

Figure S24. Time series of the 5-factor solution for Athens. The PM_1 OA composition is also shown.

Table S1. Correlation between the 4 factors in Athens and VOCs as measured by the PTR-MS.

R^2	BBOA	HOA	COA	OOA
m/z 42 (Acetonitrile)	0.81	0.67	0.35	0.20
m/z 43	0.71	0.59	0.30	0.19
m/z 47 (formic acid)	0.43	0.49	0.11	0.06
m/z 59 (acetone, glyoxal)	0.70	0.61	0.31	0.25
m/z 61 (acetic acid)	0.52	0.33	0.18	0.14
m/z 69 (isoprene, furan)	0.88	0.63	0.31	0.14
m/z 71 (MVK, MACR)	0.81	0.74	0.32	0.13
m/z 73 (MEK)	0.75	0.61	0.31	0.21
m/z 75 (hydroxyacetone)	0.69	0.41	0.24	0.09
m/z 79 (benzene)	0.71	0.70	0.31	0.16
m/z 81 (terpenes)	0.85	0.63	0.30	0.15
m/z 85 (EVK)	0.90	0.68	0.34	0.14
m/z 87 (MBO, C5, methacrylic acid)	0.93	0.59	0.33	0.15
m/z 93 (toluene)	0.37	0.54	0.18	0.09
m/z 95 (2 vinyl furan, phenol)	0.43	0.36	0.12	0.02
m/z 99 (hexenal)	0.87	0.58	0.34	0.21
m/z 101 (isoprene hyperoxides)	0.71	0.48	0.25	0.12
m/z 105(styrene)	0.54	0.55	0.19	0.09
m/z 107 (xylenes)	0.47	0.65	0.23	0.11
m/z 113 (chlorobenzene)	0.80	0.53	0.31	0.21
m/z 115 (heptanal)	0.66	0.48	0.22	0.13
m/z 121 (C9 aromatics)	0.47	0.66	0.21	0.10
m/z 129 (octanal, naphthalene)	0.70	0.73	0.21	0.07
m/z 135 (C10 aromatics)	0.50	0.64	0.21	0.12
m/z 137 (monoterpenes)	0.71	0.52	0.25	0.19
m/z 139 (nopinone)	0.67	0.41	0.22	0.18
m/z 151 (pinonaldehyde)	0.32	0.26	0.09	0.06
m/z 163 (C12 aromatics)	0.38	0.27	0.10	0.12

Table S2. Correlation between the 5 factors in Athens and VOCs as measured by the PTR-MS.

R^2	BBOA-ox	BBOA-fr	HOA	COA	OOA
m/z 42 (Acetonitrile)	0.43	0.74	0.57	0.32	0.10
m/z 43	0.43	0.63	0.53	0.28	0.09
m/z 47 (formic acid)	0.26	0.39	0.50	0.10	0.02
m/z 59 (acetone, glyoxal)	0.39	0.64	0.57	0.28	0.15
m/z 61 (acetic acid)	0.39	0.41	0.27	0.16	0.07
m/z 69 (isoprene, furan)	0.50	0.79	0.42	0.28	0.06
m/z 71 (MVK, MACR)	0.40	0.78	0.59	0.29	0.06
m/z 73 (MEK)	0.42	0.68	0.51	0.28	0.12
m/z 75 (hydroxyacetone)	0.41	0.60	0.22	0.21	0.03
m/z 79 (benzene)	0.34	0.68	0.65	0.28	0.08
m/z 81 (terpenes)	0.51	0.75	0.46	0.27	0.06
m/z 85 (EVK)	0.49	0.83	0.46	0.31	0.06
m/z 87 (MBO, C5, methacrylic acid)	0.55	0.83	0.33	0.30	0.07
m/z 93 (toluene)	0.15	0.39	0.66	0.17	0.05
m/z 95 (2 vinyl furan, phenol)	0.22	0.42	0.21	0.11	0.00
m/z 99 (hexenal)	0.52	0.76	0.39	0.31	0.10
m/z 101 (isoprene hyperoxides)	0.39	0.64	0.28	0.22	0.06
m/z 105(styrene)	0.25	0.53	0.48	0.17	0.05
m/z 107 (xylenes)	0.19	0.48	0.77	0.21	0.06
m/z 113 (chlorobenzene)	0.51	0.69	0.37	0.28	0.11
m/z 115 (heptanal)	0.38	0.60	0.32	0.20	0.06
m/z 121 (C9 aromatics)	0.20	0.48	0.76	0.20	0.06
m/z 129 (octanal, naphthalene)	0.30	0.72	0.51	0.19	0.04
m/z 135 (C10 aromatics)	0.23	0.50	0.71	0.20	0.07
m/z 137 (monoterpenes)	0.48	0.60	0.45	0.23	0.09
m/z 139 (nopinone)	0.50	0.54	0.31	0.20	0.08
m/z 151 (pinonaldehyde)	0.21	0.28	0.21	0.08	0.02
m/z 163 (C12 aromatics)	0.33	0.28	0.29	0.09	0.05

7. Comparison of BBOA and K^+ in Athens

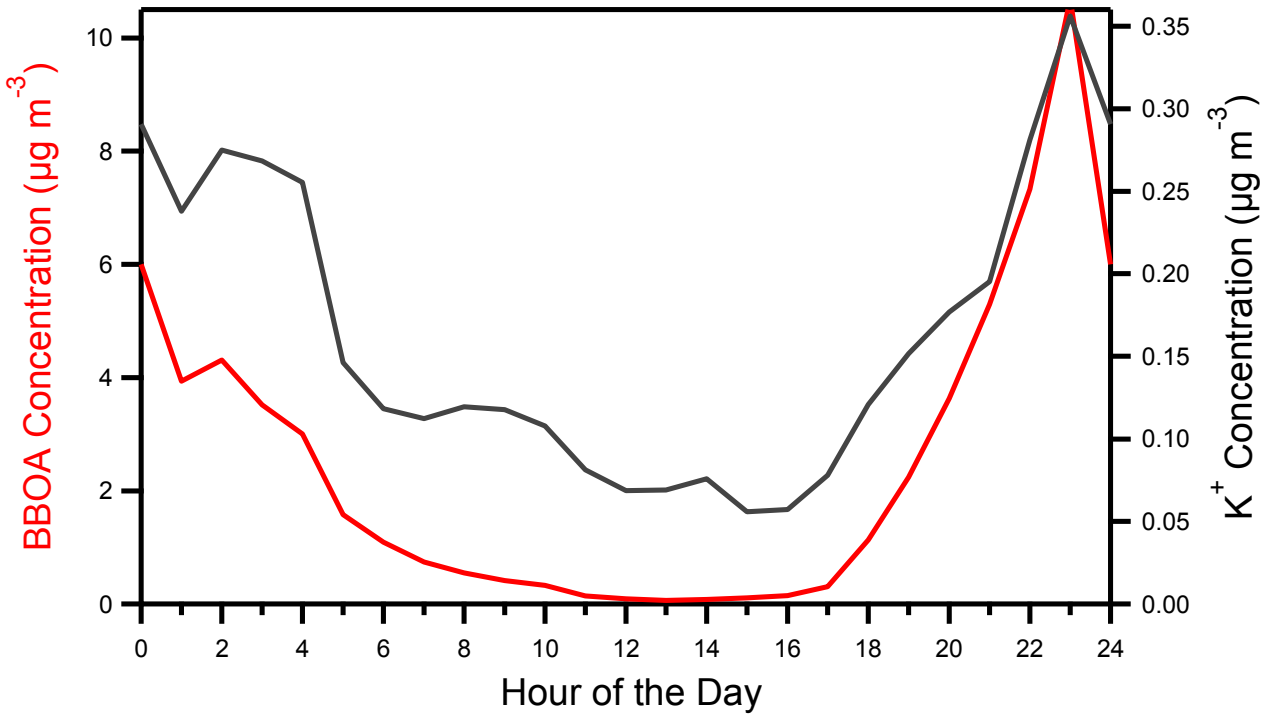

Figure S25. The diurnal profiles of the BBOA (red) and K^+ (grey) in Athens.

8. Comparison of the PMF factors' spectra for the two cities

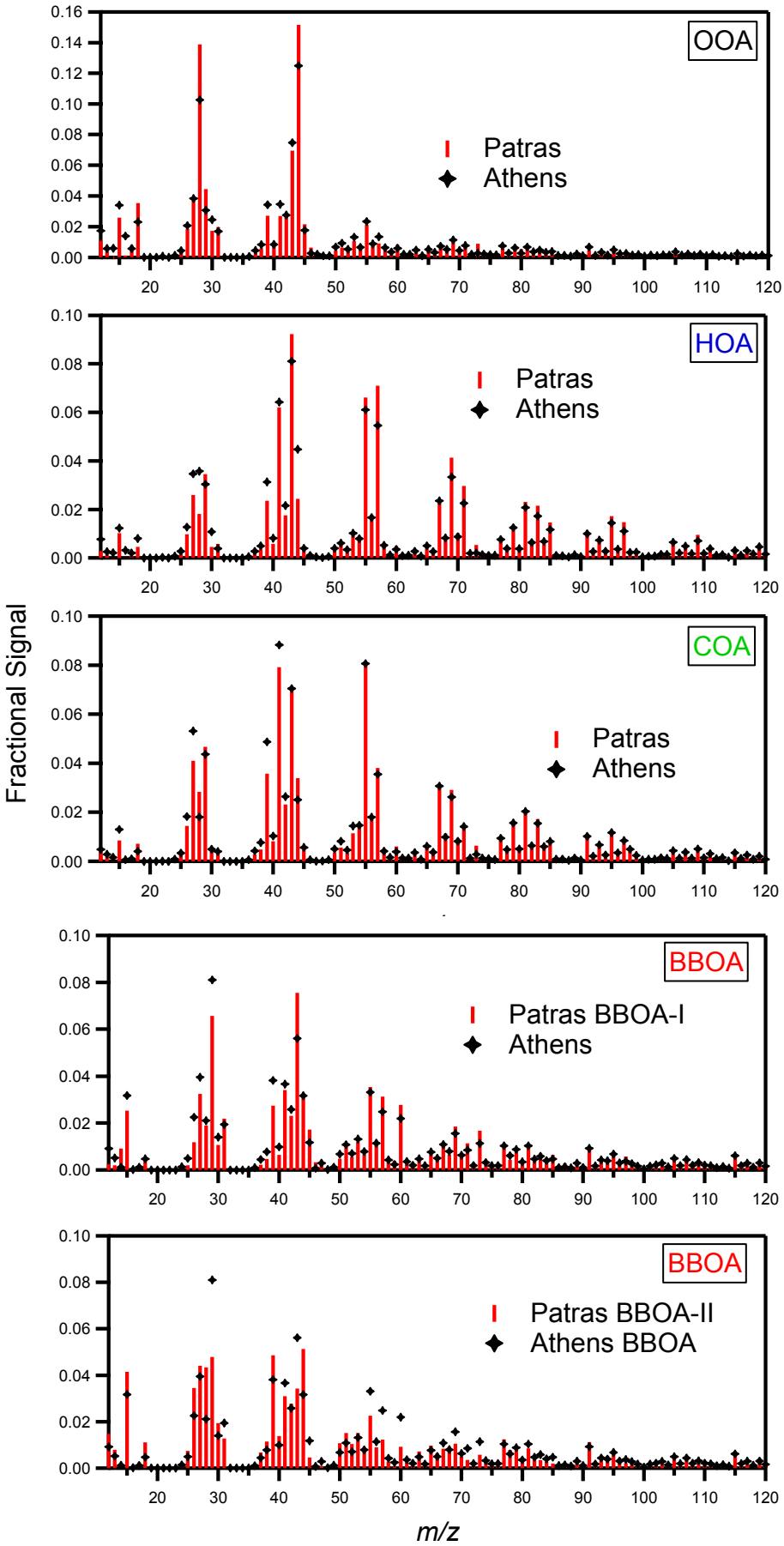

Figure S26. Comparison of the PMF-factor mass spectra for the two cities.

9. Comparison of factor spectra with other studies

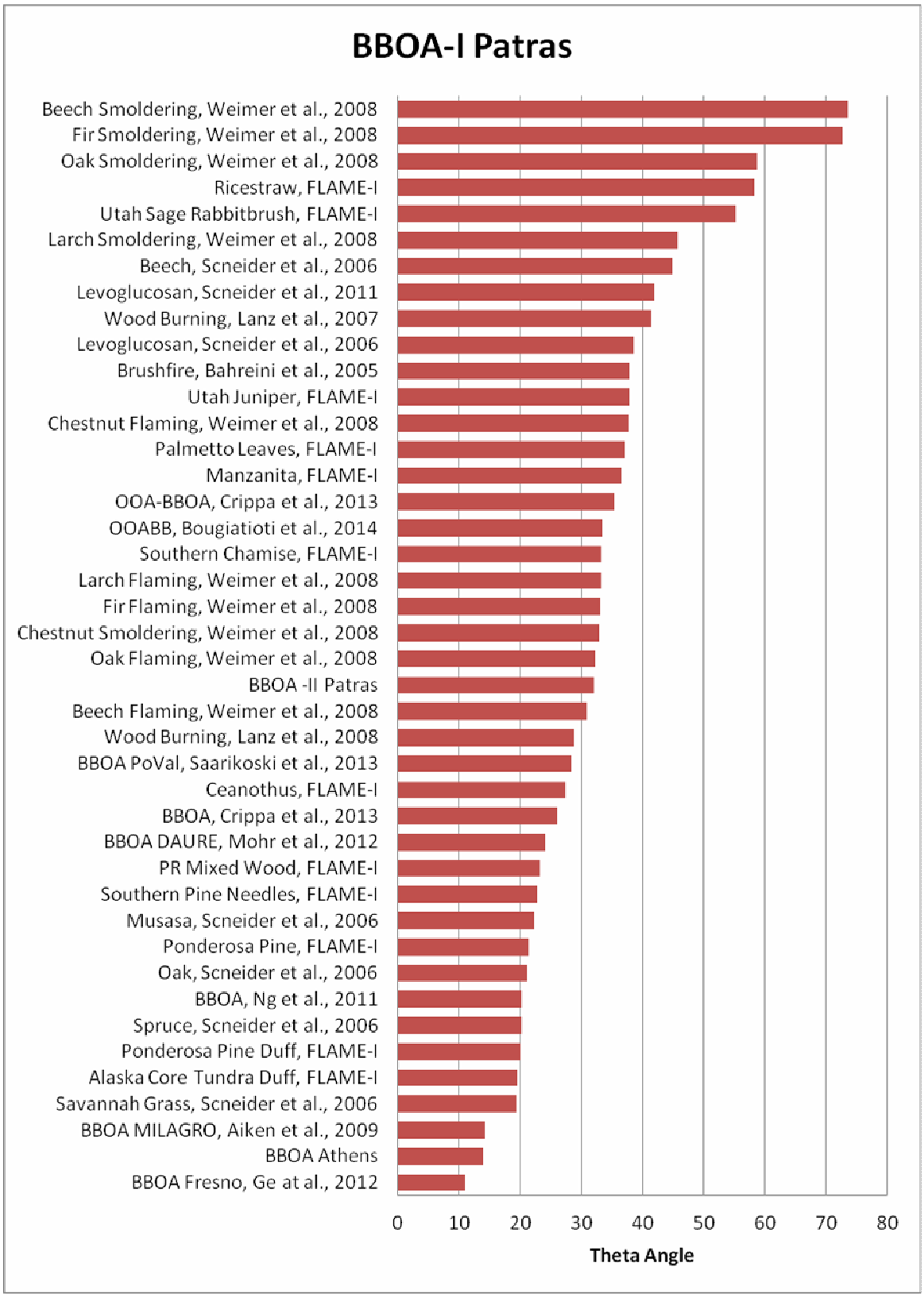

Figure S27. Theta angles between the BBOA-I mass spectra in Patras and BBOA from the literature.

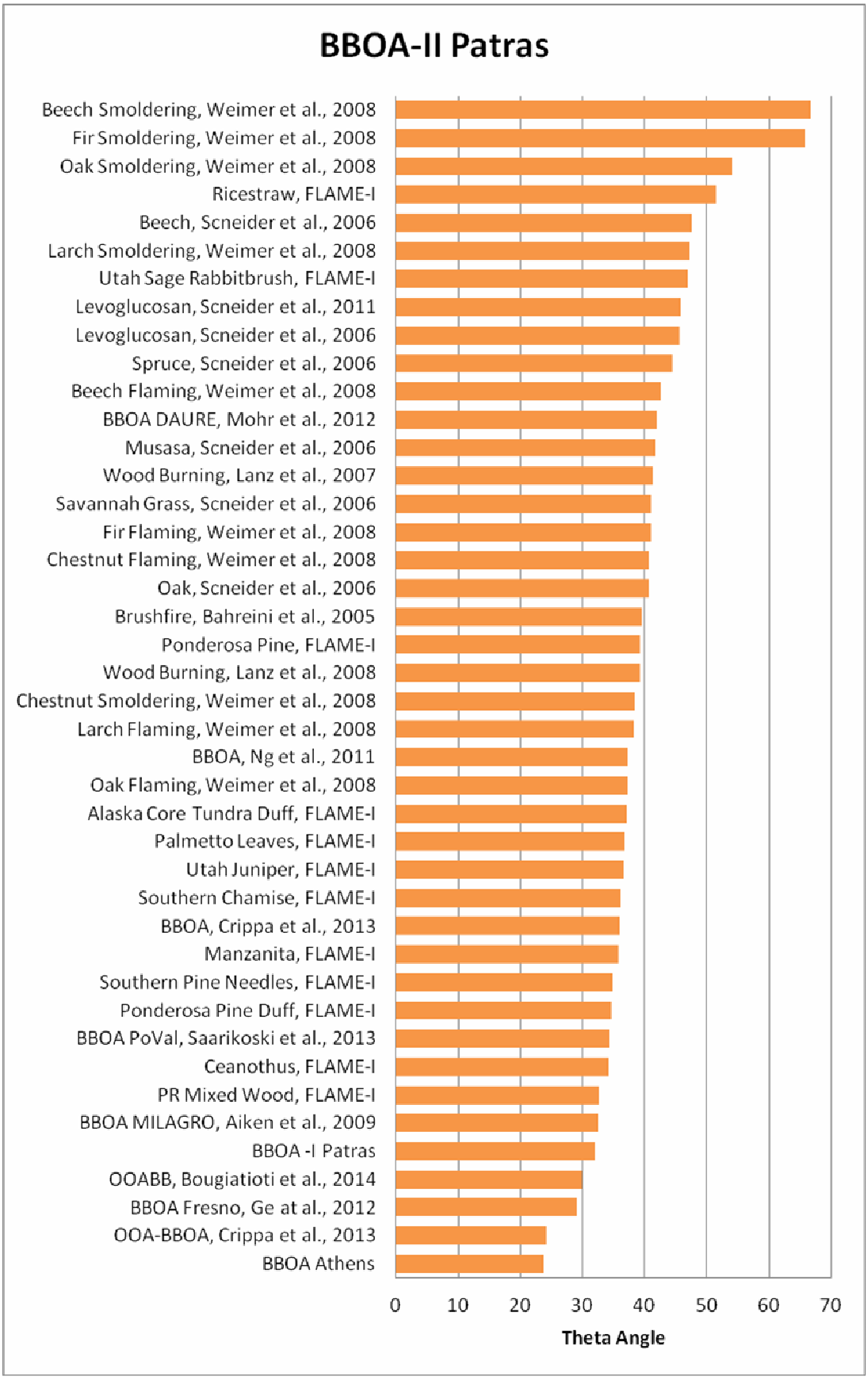

Figure S28. Theta angles between the BBOA-II mass spectra in Patras and BBOA from the literature.

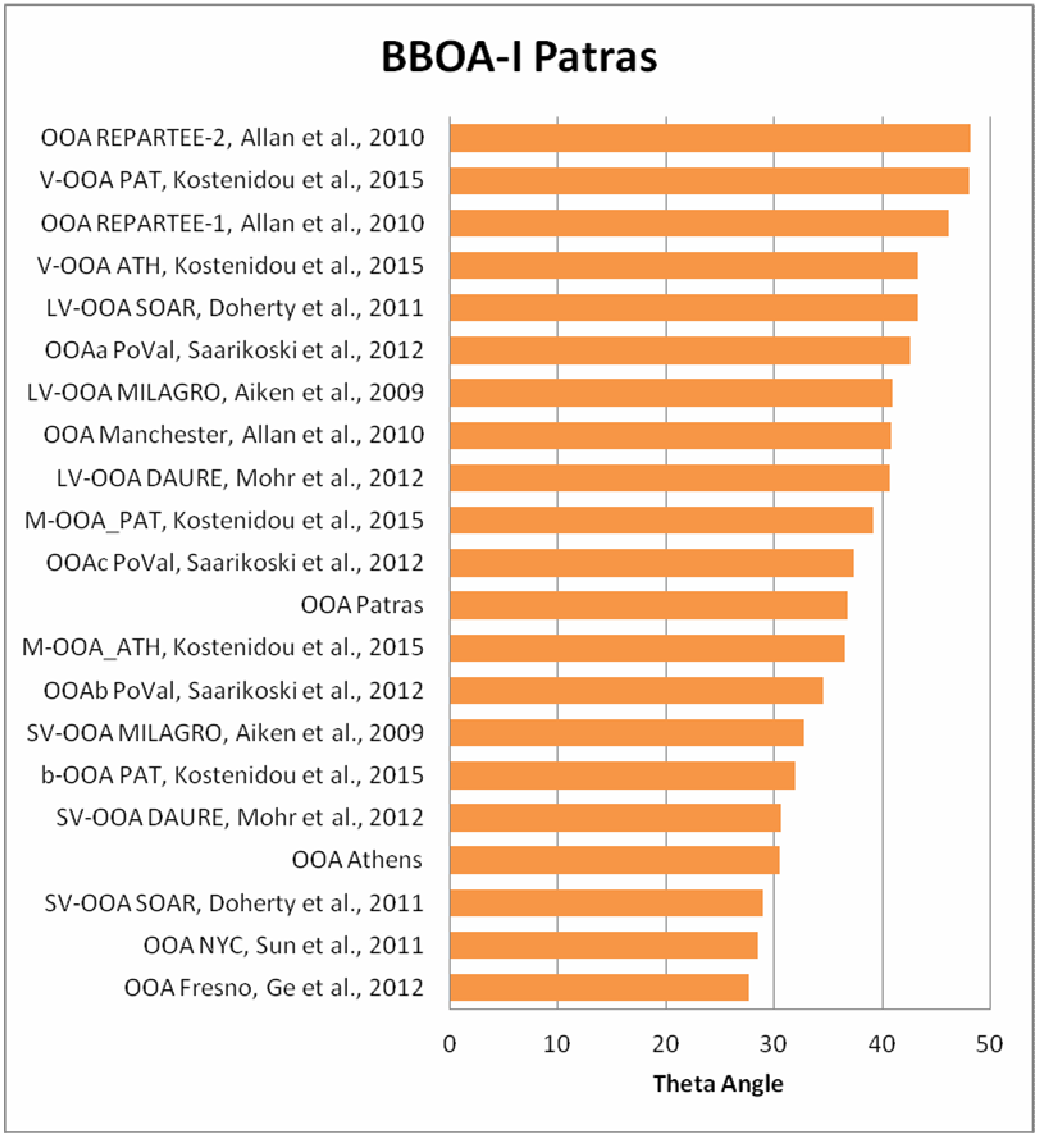

Figure S29. Theta angles between the BBOA-I mass spectra in Patras and OOA from the literature.

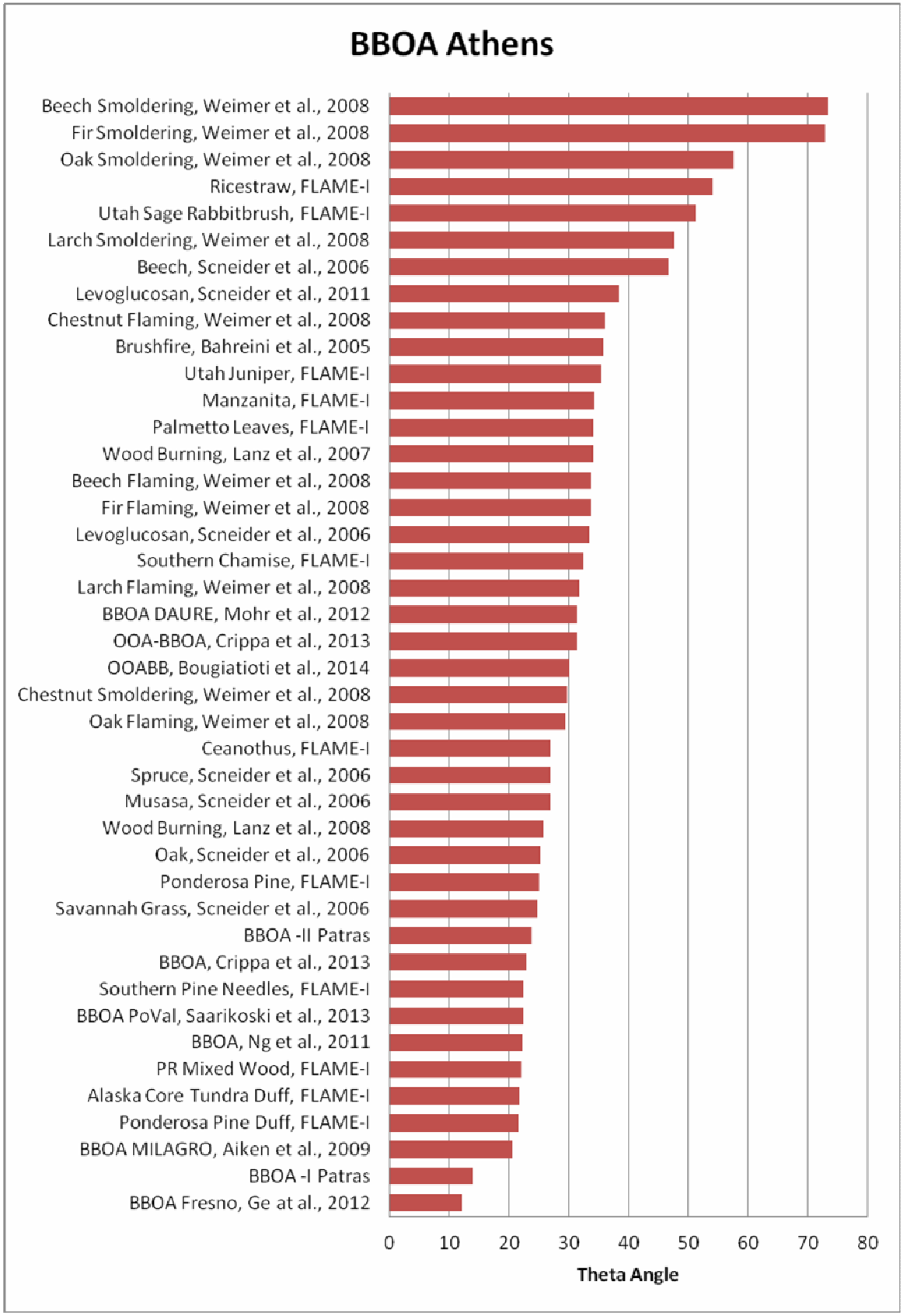

Figure S30. Theta angles between the BBOA mass spectra in Athens and BBOA spectra from the literature.

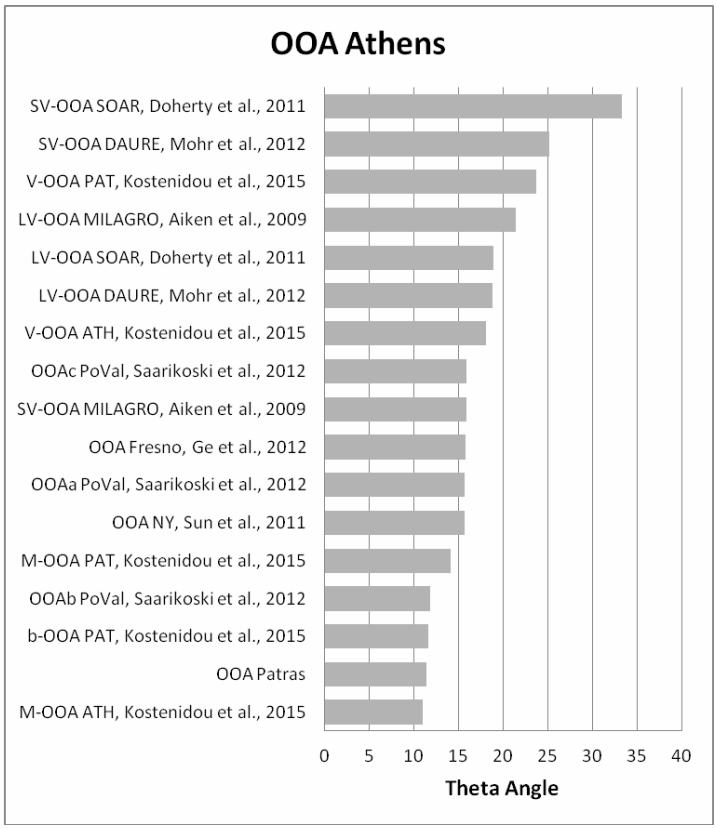

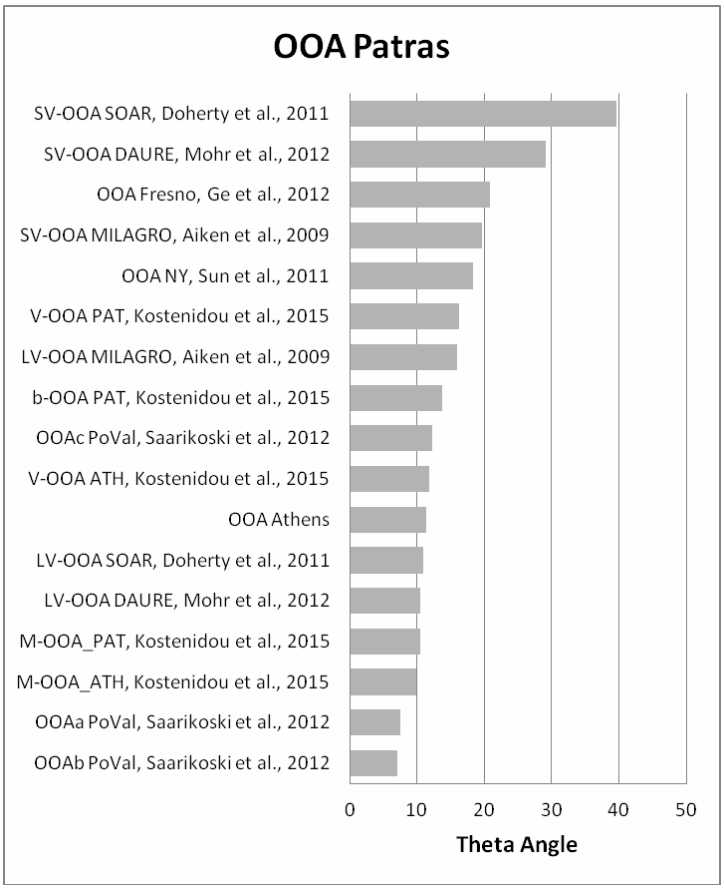

Figure S31. Theta angles between the OOA mass spectra in the two cities and the literature.

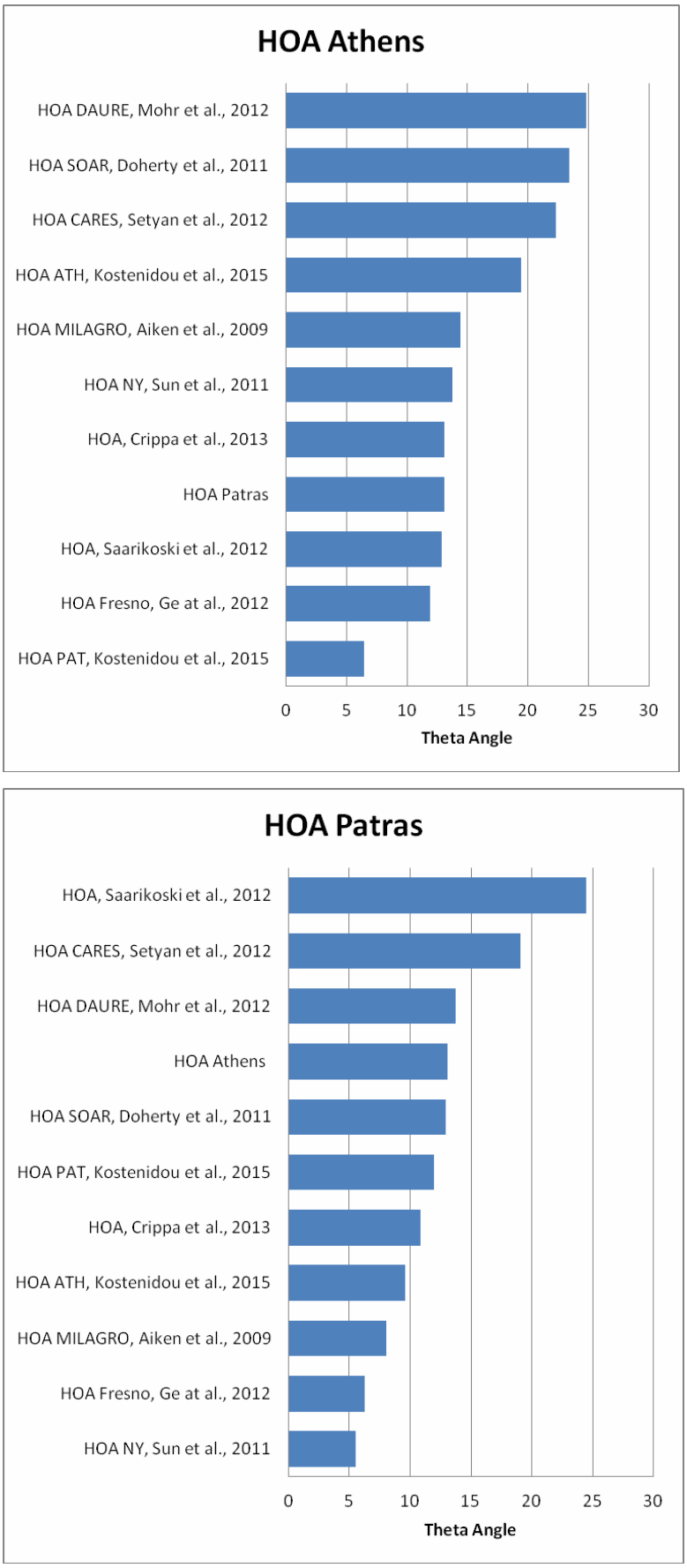

Figure S32. Theta angles between the HOA mass spectra in the two cities and the literature.

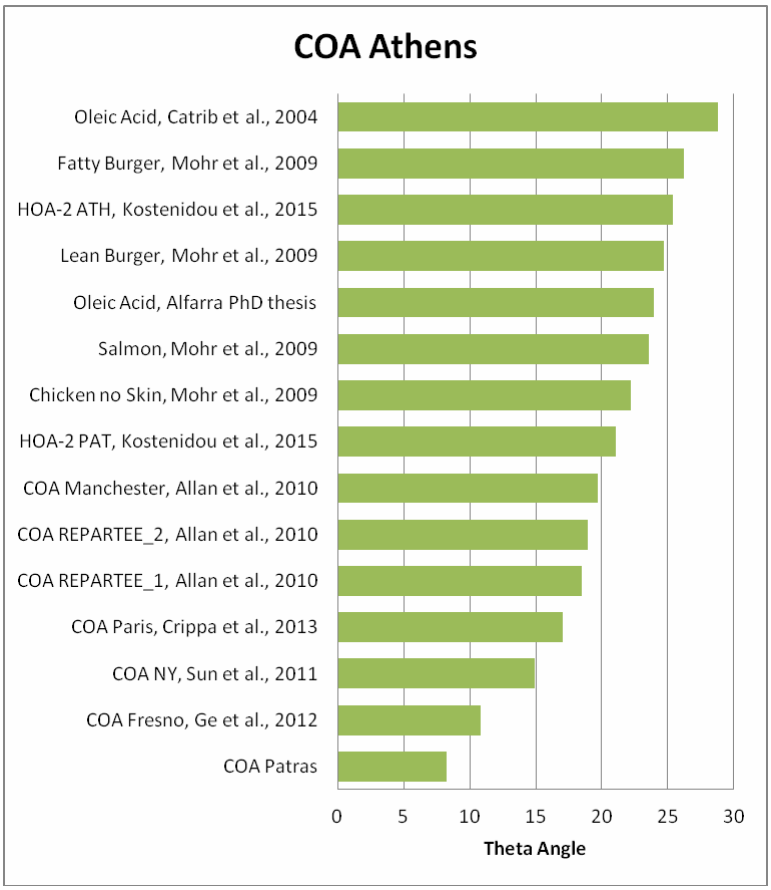

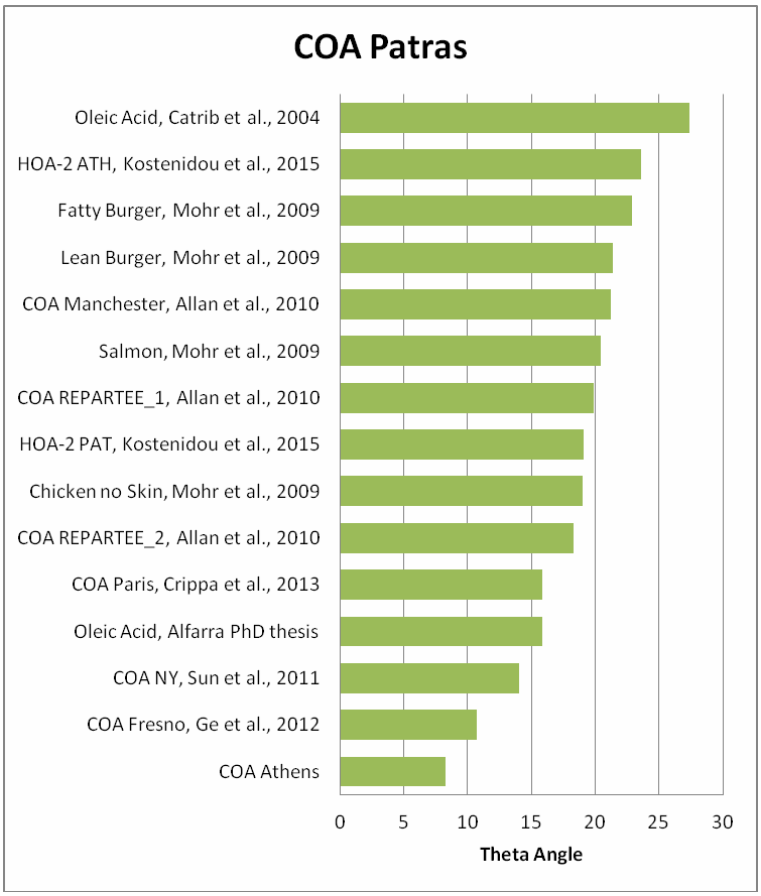

Figure S33. Theta angles between the COA mass spectra in the two cities and the literature.

10. BC and HOA

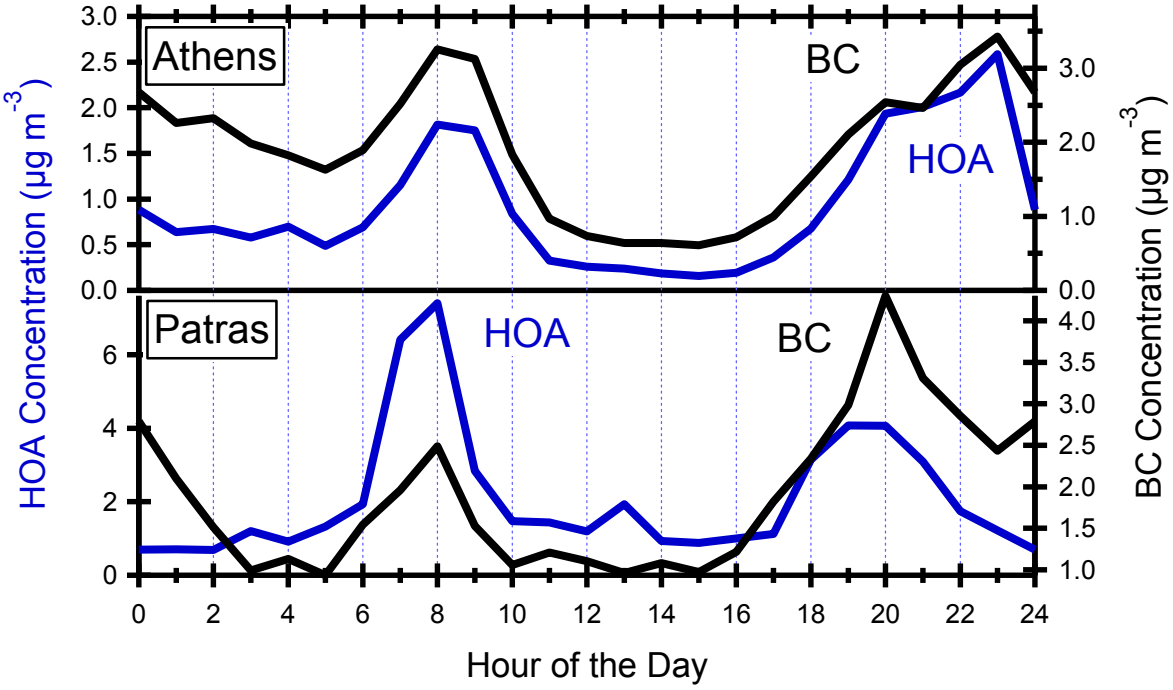

Figure S34. The diurnal profiles of the HOA and BC in a) Athens and b) Patras.

11. Ng Triangles

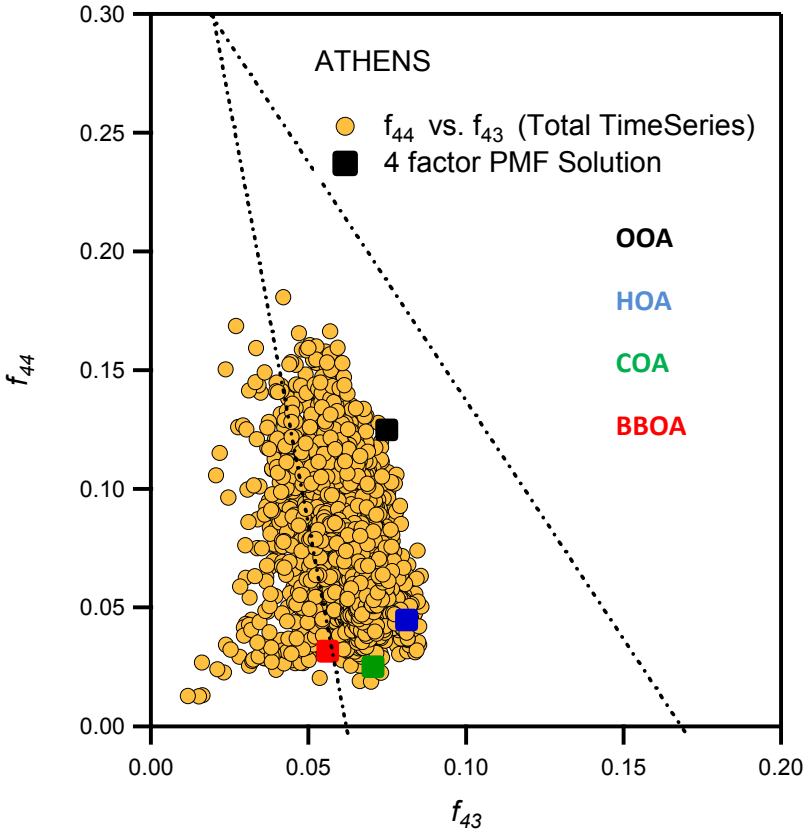

Figure S35. Ng triangle for the Athens campaign.

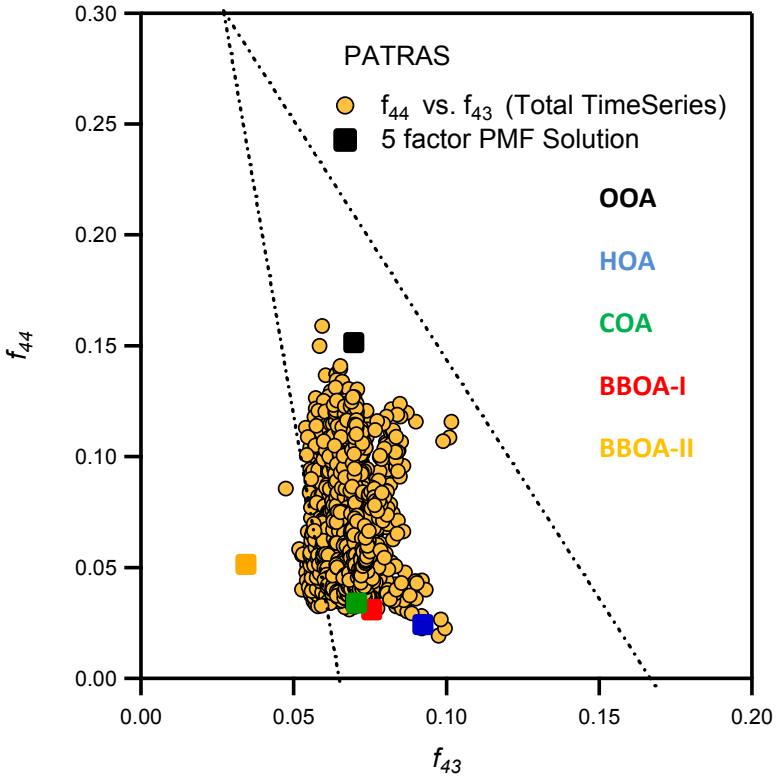

Figure S36. Ng triangle for the Patras campaign.